

Exact Mixed-integer Convex Programming Formulation for Optimal Water Network Design

Byron Tasseff

Information Systems and Modeling, Los Alamos National Laboratory, Los Alamos, NM 87545, btasseff@lanl.gov
Department of Industrial and Operations Engineering, University of Michigan, Ann Arbor, MI 48109

Russell Bent

Applied Mathematics and Plasma Physics, Los Alamos National Laboratory, Los Alamos, NM 87545

Marina A. Epelman

Department of Industrial and Operations Engineering, University of Michigan, Ann Arbor, MI 48109

Donatella Pasqualini

Information Systems and Modeling, Los Alamos National Laboratory, Los Alamos, NM 87545

Pascal Van Hentenryck

H. Milton Stewart School of Industrial and Systems Engineering, Georgia Institute of Technology, Atlanta, GA 30332

In this paper, we consider the canonical water network design problem, which contains nonconvex potential loss functions and discrete resistance choices with varying costs. Traditionally, to resolve the nonconvexities of this problem, relaxations of the potential loss constraints have been applied to yield a more tractable mixed-integer convex program (MICP). However, design solutions to these relaxed problems may not be feasible with respect to the full nonconvex physics. In this paper, it is shown that, in fact, the original mixed-integer nonconvex program can be reformulated *exactly* as an MICP. Beginning with a convex program previously used for proving nonlinear network design feasibility, strong duality is invoked to construct a novel, convex primal-dual system embedding all physical constraints. This convex system is then augmented to form an exact MICP formulation of the original design problem. Using this novel MICP as a foundation, a global optimization algorithm is developed, leveraging heuristics, outer approximations, and feasibility cutting planes for infeasible designs. Finally, the algorithm is compared against the previous relaxation-based state of the art in water network design over a number of standard benchmark instances from the literature.

Key words: mixed-integer nonlinear programming, network optimization, potable water distribution

1. Introduction

This paper considers the problem of optimal water network design, where the layout of the network is known, and the diameter and material of each pipe must be selected from a discrete set to

minimize cost while satisfying fixed demand. The canonical design problem presented throughout the literature excludes common operational components (e.g., pumps), and all demand is assumed to be gravity-fed. This paper focuses on the development of mathematical programming (non-heuristic) solution techniques for this problem. However, because of the nonconvexities that appear in the physics of water systems, naive mathematical programming formulations quickly become intractable. To address this, the problem is typically relaxed via convexification. Unfortunately, solutions to these relaxed problems may be infeasible with respect to the full nonconvex physics.

To this end, Cherry (1951) introduced a convex program for determining the feasibility of a fixed network governed by linear conservation laws and nonlinear potential loss relationships. Raghunathan (2013) later revisited this model, using it as a simple tool within a global, relaxation-based design optimization algorithm. However, the greater potential of a *convex* description for feasibility has gone, for the most part, surprisingly overlooked. This paper explores this potential, which ultimately provides a new understanding of water network design. Its contributions include

- A convex embedding of *all* physical constraints for a feasible network design;
- An *exact* mixed-integer convex reformulation of the optimal design problem;
- Development of a new global, relaxation-based algorithm for optimal network design;
- A comparison of this algorithm with the previous state of the art (Raghunathan 2013);
- New lower and upper bounds for open benchmark instances throughout the literature.

More broadly, these contributions could be further generalized to optimal network design and expansion planning problems for other important network types exhibiting nonlinear relationships among nodal potentials and flows (e.g., natural gas and crude oil transmission networks).

As background, Section 2 reviews optimization techniques for water and other similar network problems, Section 3 formulates the water network design problem as a mixed-integer nonconvex program, and Section 4 summarizes the contributions of Raghunathan (2013): (i) their mixed-integer convex programming (MICP) relaxation, (ii) the further relaxation that forms a mixed-integer linear program (MIP), and (iii) the outline of a MIP-based algorithm. The remaining sections

detail this paper’s contributions: Section 5 derives a convex description of feasible designs, then reformulates the optimal design problem *exactly* as an MICP; Section 6 augments Raghunathan’s algorithm with novel outer approximations based on the new MICP; Section 7 compares the new and previous algorithms using instances from the literature; and Section 8 concludes the paper.

2. Literature Review

Nonlinear networks refer to a class of networks in which (i) flow is driven by potentials and (ii) potential loss along an edge is a nonlinear function of flow. Network types with these properties include potable water, natural gas, and crude oil. Because of their mathematically similar descriptions, optimization methods developed for any of these networks are often easily adapted to the others. For over fifty years, a variety of techniques have been employed to solve optimization problems that involve these network types (Raghunathan 2013). Mala-Jetmarova et al. (2017, 2018) provide comprehensive literature reviews of solution techniques used for optimal water network operation and design, both of which are dominated by metaheuristic methods. Ríos-Mercado and Borraz-Sánchez (2015) provide a similar review of techniques for problems involving natural gas networks. Finally, Sahebi et al. (2014) review methods for optimizing crude oil supply chains.

Outside of mathematical programming, the predominant approaches used for solving water network design problems have been heuristic techniques based on simulation optimization. Indeed, as Mala-Jetmarova et al. (2018) express, “... research [has] been trapped, to some extent, in applying new metaheuristic [optimization] methods to relatively simple (from an engineering perspective) design problems, without understanding the principles behind algorithm performance.” The same review specifies that 84% of the 124 studies compared use “stochastic” methods (e.g., evolutionary and genetic algorithms), 9% use “deterministic” methods (e.g., linear and nonlinear programming), and 7% use hybridized methods. Maier et al. (2015) similarly describe the prevalence of metaheuristic optimization techniques in the water resources literature and their associated performance inconsistencies. For these reasons, as well as due to the lack of optimality guarantees associated with

metaheuristic techniques, this paper instead focuses on mathematical programming (specifically, globally optimal mixed-integer nonlinear) approaches for solving water network design problems.

A number of recent studies have developed mathematical programming techniques that have proven to be effective on various nonlinear network problems. Borraz-Sánchez et al. (2016) develop a relaxation-based method for natural gas network expansion planning. D’Ambrosio et al. (2015) provide a survey of methods used throughout water system optimization, which includes both approximation- and relaxation-based techniques for optimal water network operation and design. Raghunathan (2013) presents a relaxation-based approach for general nonlinear network design and showcases its efficacy on water network design instances. Our paper considers the algorithm therein to be the state of the art for global nonlinear network design. As such, their algorithm serves as a foundation for the one developed in this paper, where only the selection of cuts differs.

In conjunction with recent advances in relaxation-based methods for optimizing over nonlinear networks, similar developments have been made in formulating cuts that strengthen these relaxations. Humpola and Fügenschuh (2013) develop a number of valid inequalities for nonlinear network design problems and briefly describe their potential for water networks. Humpola et al. (2016) extend this work for natural gas. In both cases, valid cuts are derived from the solution of a nonconvex program and several auxiliary problems. In contrast, the cuts in this paper are trivially derived from the novel mixed-integer convex reformulation of the original network design problem.

Finally, the notion of a convex feasibility problem for nonlinear networks, originating with Cherry (1951) and exploited computationally by Raghunathan (2013), is also discussed by De Wolf and Smeers (1994). Here, a convex reformulation of the optimal natural gas transmission problem under restrictive assumptions is presented. A number of properties of this problem are then described, including solution uniqueness and physical interpretation. Unlike this paper, however, the problem they consider is not discrete, and their contributions appear to have gone unused throughout the natural gas optimization literature. Moreover, their work derives the reformulation via variational inequality theory, whereas this paper obtains a more general formulation via Lagrangian duality.

3. Problem Formulation

3.1. Notation for Sets

A water distribution network is represented by a directed graph $\mathcal{G} := (\mathcal{N}, \mathcal{A})$, where \mathcal{N} is the set of nodes (i.e., junctions and reservoirs) and \mathcal{A} is the set of arcs (i.e., pipes). Herein, the set of reservoirs (i.e., source nodes with fixed potentials) is denoted by $\mathcal{S} \subset \mathcal{N}$ and the set of junctions by $\mathcal{J} \subset \mathcal{N}$. Junctions are modeled as demand nodes (where the demand for flow is nonnegative) and, without loss of generality, $\mathcal{S} \cap \mathcal{J} = \emptyset$. The set of arcs incident to node $i \in \mathcal{N}$ where i is the tail (respectively, head) of the arc is denoted by $\delta_i^+ := \{(i, j) \in \mathcal{A}\}$ (respectively, $\delta_i^- := \{(j, i) \in \mathcal{A}\}$). All arcs incident to a source node $i \in \mathcal{S}$ are assumed to be outgoing, i.e., $\delta_i^- = \emptyset$ and $\delta_i^+ \neq \emptyset$, and arcs with tails at demand nodes $i \in \mathcal{J}$ have heads also at demand nodes. Finally, the design problem of Section 3.3 involves selecting from a set of resistances $\mathcal{R}_a := \{p_1, p_2, \dots, p_{|\mathcal{R}_a|}\}$ for each $a \in \mathcal{A}$.

3.2. Physical Feasibility

This section describes the variables and constraints required to model the physics of gravity-fed water networks given a *fixed* selection of pipe resistances r_a , $a \in \mathcal{A}$. In the constraints that follow, q_a , $a \in \mathcal{A}$, denote variables representing the flow of water across each arc (expressed as a volumetric flow rate in m³/s). Nodal potentials are denoted by the variables h_i , $i \in \mathcal{N}$, where each represents the total hydraulic head in units of length (m). The total hydraulic head (hereafter referred to as “head”) assimilates elevation and pressure heads at a node, while the velocity head is neglected.

Flow Bounds When q_a is positive (negative), flow on arc $a := (i, j)$ travels from node i to j (j to i). Flow is often bounded by physical capacity, engineering judgment, or network analysis. Herein,

$$\underline{q}_a \leq q_a \leq \bar{q}_a, \forall a \in \mathcal{A}. \quad (1)$$

For example, the maximum speed of flow along arc $a \in \mathcal{A}$, \bar{v}_a , is often used to estimate the bounds $\underline{q}_a = -\frac{\pi}{4}\bar{v}_a D_a^2$ and $\bar{q}_a = \frac{\pi}{4}\bar{v}_a D_a^2$, where D_a is the fixed diameter of the pipe indexed by $a \in \mathcal{A}$.

Head Bounds For each reservoir $i \in \mathcal{S}$, the head is fixed at a constant value h_i^s , i.e.,

$$h_i = h_i^s, \forall i \in \mathcal{S}. \quad (2)$$

For each junction $i \in \mathcal{J}$, a predefined minimum head \underline{h}_i must be satisfied. Upper bounds on heads can also be provided or implied by network data. For example, this paper assumes

$$\underline{h}_i \leq h_i \leq \bar{h}_i = \max_{j \in \mathcal{S}} \{h_j^s\}, \forall i \in \mathcal{J}. \quad (3)$$

Conservation of Flow at Demand Nodes Flow must be delivered throughout the network in order to satisfy fixed nonnegative demand, d_i , at all demand nodes $i \in \mathcal{J}$. That is,

$$\sum_{a \in \delta_i^-} q_a - \sum_{a \in \delta_i^+} q_a = d_i, \forall i \in \mathcal{J}. \quad (4)$$

Head Loss Relationships In water networks, flow along an arc is induced by the difference in head between the two nodes connected by that arc. The relationships that link flow and head are commonly referred to as the “head loss equations” and are generally of the form

$$h_i - h_j = \phi_a(q_a), \forall a := (i, j) \in \mathcal{A}, \quad (5)$$

where $\phi_a : \mathbb{R} \rightarrow \mathbb{R}$ is a strictly increasing function with rotational symmetry about the origin. The most common head loss relationships include the Darcy-Weisbach equation,

$$h_i - h_j = \frac{8L_a\tau_a q_a |q_a|}{\pi^2 g D_a^5}, \quad (6)$$

and the Hazen-Williams equation (where the constant 10.7 is in standard units),

$$h_i - h_j = \frac{10.7 L_a q_a |q_a|^{0.852}}{\kappa_a^{1.852} D_a^{4.8704}}. \quad (7)$$

Here, L_a is the pipe length, τ_a is the friction factor, g is gravitational acceleration, and κ_a is the roughness, which depends on the pipe material. In Equation (6), τ_a depends on q_a in a nonlinear manner. However, in the mathematical programming literature, τ_a is often fixed to a constant, which removes the term’s nonlinearity in q_a (Gleixner et al. 2012, Verleye and Aghezzaf 2013).

When all terms *except* h_i , h_j , and q_a are fixed, both head loss equations reduce to

$$h_i - h_j = L_a r_a q_a |q_a|^{\alpha-1}, \forall a := (i, j) \in \mathcal{A}. \quad (8)$$

Here, α denotes the exponent required by Equation (6) or (7) (i.e., 2 or 1.852, respectively), and r_a , $a \in \mathcal{A}$, denotes the resistance per unit length. The resistance per unit length comprises all non-length constant terms appearing in Equations (6) and (7) and is in units of $(\text{m}^3/\text{s})^{-\alpha}$.

For fixed resistances r , the nonconvex formulation for water network feasibility is thus

Physical bounds: Constraints (1), (2), (3)

Flow conservation: Constraints (4) (NLP(r))

Head loss relationships: Constraints (8).

3.3. Optimal Network Design

To formulate the design problem, (NLP(r)) is coupled with the combinatorial problem of selecting one resistance from a predefined set of resistances for each arc, \mathcal{R}_a for $a \in \mathcal{A}$, while minimizing the overall cost of network design. To model the disjunction representing discrete resistance choices, each q_a is first decomposed into $|\mathcal{R}_a|$ binary variables x_{ap} and continuous variables q_{ap} , i.e.,

$$q_a := \sum_{p \in \mathcal{R}_a} q_{ap}, \quad \forall a \in \mathcal{A}, \quad (9)$$

$$\underline{q}_{ap} x_{ap} \leq q_{ap} \leq \bar{q}_{ap} x_{ap}, \quad x_{ap} \in \mathbb{B}, \quad \forall a := (i, j) \in \mathcal{A}, \quad \forall p \in \mathcal{R}_a. \quad (10)$$

Here, $x_{ap} = 1$ when $p \in \mathcal{R}_a$ is selected and zero otherwise. From Constraint (10), it follows that q_{ap} is nonzero only when $x_{ap} = 1$. Also note that $\underline{q}_{ap} = -\frac{\pi}{4} \bar{v}_a D_{ap}^2$ and $\bar{q}_{ap} = \frac{\pi}{4} \bar{v}_a D_{ap}^2$ are often used as bounds, as each $p \in \mathcal{R}_a$ is typically derived from a unique pipe diameter D_{ap} . Since only one resistance may be selected per pipe indexed by $a \in \mathcal{A}$, we include the additional constraints

$$\sum_{p \in \mathcal{R}_a} x_{ap} = 1, \quad \forall a \in \mathcal{A}. \quad (11)$$

The head loss Constraints (8) are then expanded to formulate the constraints

$$h_i - h_j = L_a \sum_{p \in \mathcal{R}_a} p q_{ap} |q_{ap}|^{\alpha-1}, \quad \forall a := (i, j) \in \mathcal{A}. \quad (12)$$

Finally, the objective function, $\eta(x)$, for the optimal design problem is written as

$$\eta(x) = \sum_{a \in \mathcal{A}} L_a \sum_{p \in \mathcal{R}_a} c_{ap} x_{ap}, \quad (13)$$

where c_{ap} is the cost per unit length of installing a pipe along $a \in \mathcal{A}$ with resistance $p \in \mathcal{R}_a$.

These modifications allow the optimal water network design problem to be written as

$$\begin{aligned}
 & \text{minimize} && \text{Objective function: } \eta(x) \text{ of Equation (13)} \\
 & \text{subject to} && \text{Physical bounds: Constraints (2), (3), (10)} \\
 & && \text{Flow conservation: Constraints (4)} && \text{(MINLP)} \\
 & && \text{Resistance selection: Constraints (11)} \\
 & && \text{Head loss relationships: Constraints (12)}.
 \end{aligned}$$

Here, Constraints (4) employ the definitions of q_a described in Equations (9). Note that (MINLP) is mixed-integer *nonconvex* because of the nonconvex Constraints (12). Raghunathan (2013) addresses this challenge via a convex relaxation of the complicating constraints, followed by linearization of the resulting MICP. Their method is reviewed in Section 4. This paper, on the other hand, addresses this challenge via an *exact* convex reformulation of (NLP(r)) to describe feasibility, followed by an *exact* MICP reformulation of (MINLP). These are further described in Section 5.

4. Relaxation-based Reformulation and Algorithm

This section reviews the methods of Raghunathan (2013), which this paper uses as its foundations. First, their relaxed MICP of the design problem is presented in Section 4.1. Then, an exact MIP reformulation of (MINLP), based on an outer approximation of the MICP, is presented in Section 4.2. A convex program for determining the feasibility of a design is presented in Section 4.3. Finally, a simple global algorithm, which leverages the relaxed MIP formulation described in Section 4.2, is presented in Section 4.4. These details prepare the reader for *this study's exact* MICP reformulation described in Section 5, as well as for the relaxation-based global algorithm presented in Section 6.

4.1. Mixed-integer Convex Relaxation of (MINLP)

This section relaxes the nonconvex head loss constraints of (MINLP) via an outer convexification to form a relaxed MICP of the original optimal design problem. This is accomplished by partitioning

Constraints (12) into their symmetric positive and negative components. To begin, variables q_{ap}^\pm are introduced, denoting nonnegative flows in the two directions along arc $a \in \mathcal{A}$, with

$$q_a := \sum_{p \in \mathcal{R}_a} (q_{ap}^+ - q_{ap}^-), \quad \forall a \in \mathcal{A} \quad (14)$$

replacing Equations (9). Next, the bound Constraints (10) in (MINLP) are rewritten as

$$0 \leq q_{ap}^\pm \leq \bar{q}_{ap}^\pm x_{ap}, \quad x_{ap} \in \mathbb{B}, \quad \forall a \in \mathcal{A}, \quad \forall p \in \mathcal{R}_a, \quad (15)$$

where $\bar{q}_{ap}^+ = \max\{0, \bar{q}_{ap}\}$ and $\bar{q}_{ap}^- = \max\{0, -\underline{q}_{ap}\}$ replace the bounds of Constraints (10). Nonnegative head difference variables Δh_a^\pm are similarly introduced to denote head loss in the two possible flow directions. These are related to the original head variables $h_i, i \in \mathcal{N}$, via the constraints

$$\Delta h_a^+ - \Delta h_a^- = h_i - h_j, \quad \forall a := (i, j) \in \mathcal{A}. \quad (16)$$

Next, binary variables $y_a \in \mathbb{B}, a \in \mathcal{A}$, are introduced to denote the direction of flow along each arc, where, for $a = (i, j)$, $y_a = 1$ implies flow from i to j and $y_a = 0$ implies flow from j to i , i.e.,

$$0 \leq q_{ap}^+ \leq \bar{q}_{ap}^+ y_a, \quad 0 \leq q_{ap}^- \leq \bar{q}_{ap}^- (1 - y_a), \quad y_a \in \mathbb{B}, \quad \forall a \in \mathcal{A}, \quad \forall p \in \mathcal{R}_a \quad (17a)$$

$$0 \leq \Delta h_a^+ \leq \Delta \bar{h}_a^+ y_a, \quad 0 \leq \Delta h_a^- \leq \Delta \bar{h}_a^- (1 - y_a), \quad y_a \in \mathbb{B}, \quad \forall a \in \mathcal{A}. \quad (17b)$$

Here, each head difference bound $\Delta \bar{h}_a^\pm$ is derived from the lower and upper bounds on h in Constraints (3). Next, the right-hand sides in Equations (8) are decomposed into two convex functions representing head loss in the positive and negative directions. This decomposition implies

$$\Delta h_a^\pm = L_a \sum_{p \in \mathcal{R}_a} p (q_{ap}^\pm)^\alpha, \quad \forall a \in \mathcal{A}. \quad (18)$$

Recalling that q_{ap}^\pm 's can be nonzero for only one $p \in \mathcal{R}_a$, Equations (18) are then relaxed as

$$L_a p (q_{ap}^\pm)^\alpha \leq \Delta h_a^\pm, \quad \forall a \in \mathcal{A}, \quad \forall p \in \mathcal{R}_a. \quad (19)$$

Note that $(0, 0)$ and $(\bar{q}_{ap}^\pm, L_a p (\bar{q}_{ap}^\pm)^\alpha)$ are endpoints of the lines that upper-bound the strictly convex right-hand terms of Equations (18), with the slopes of these lines calculated as $\frac{L_a p (\bar{q}_{ap}^\pm)^\alpha - 0}{\bar{q}_{ap}^\pm - 0} = L_a p (\bar{q}_{ap}^\pm)^{\alpha-1}$. The convex relaxations in Constraints (19) are then linearly upper-bounded via

$$\Delta h_a^\pm \leq L_a \sum_{p \in \mathcal{R}_a} \left[p (\bar{q}_{ap}^\pm)^{\alpha-1} q_{ap}^\pm \right], \quad \forall a \in \mathcal{A}. \quad (20)$$

These constraints give rise to an MICP *relaxation* of (MINLP), namely,

$$\begin{aligned}
& \text{minimize} && \text{Objective function: } \eta(x) \text{ of Equation (13)} \\
& \text{subject to} && \text{Physical bounds: Constraints (2), (3), (15)} \\
& && \text{Flow conservation: Constraints (4)} \\
& && \text{Resistance selection: Constraints (11)} \\
& && \text{Head difference relationships: Constraints (16), (19), (20)} \\
& && \text{Direction-related inequalities: Constraints (17)}.
\end{aligned} \tag{MICP-R}$$

Here, Constraints (4) employ the definitions of q_a described in Equations (14). The validity of this relaxed formulation was proven by Raghunathan (2013). However, note that because (MICP-R) is a relaxation of (MINLP), network design solutions that are feasible to (MICP-R) may not be feasible with respect to the original, nonconvex head loss constraints of (MINLP).

4.2. Mixed-integer Linear Reformulation of (MINLP)

Raghunathan (2013) solves (MINLP) via a global, relaxation-based MIP algorithm. The algorithm leverages much of (MICP-R), linear outer approximations of Constraints (19), and linear feasibility cuts for integer solutions \hat{x} that are infeasible to (MINLP). This section restates these cuts, then develops a MIP reformulation of (MINLP), representing Raghunathan's theoretical contributions.

Outer Approximation Cutting Planes Since Constraints (19) are convex, they are easily linearized via outer approximation. However, instead of applying traditional first-order outer approximations for *each* Constraint (19), Raghunathan (2013) derives aggregate outer approximations based on the notion of outer-approximating lines with *equal intercepts* for all $p \in \mathcal{R}_a$. This is illustrated in Figure 1 for an instance where $|\mathcal{R}_a| = 3$ and $r_a = p_2$. Note that a standard outer approximation of Constraint (19) for $p \in \mathcal{R}_a$, based on the first-order Taylor expansion of its left-hand side at \tilde{q}_{ap}^\pm , is

$$(1 - \alpha) L_a p (\tilde{q}_{ap}^\pm)^\alpha + \alpha L_a p (\tilde{q}_{ap}^\pm)^{\alpha-1} q_{ap}^\pm \leq \Delta h_a^\pm. \tag{21}$$

Thus, if we fix a point $\tilde{q}_{ar_a}^\pm \in [0, \bar{q}_{ar_a}^\pm]$ for some chosen $r_a \in \mathcal{R}_a$ and $a \in \mathcal{A}$, for the remaining $p \in \mathcal{R}_a$, the outer approximations will have the *same constant intercept* for $\tilde{q}_{ap}^\pm := \tilde{q}_{ar_a}^\pm (r_a/p)^{1/\alpha}$.

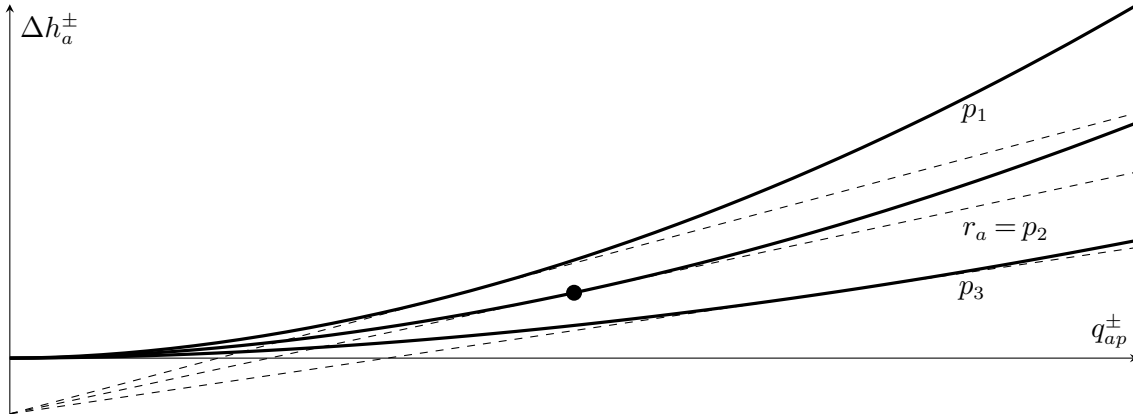


Figure 1 Depiction of equal intercept outer approximations (dashed) of convexified head loss relations (solid) for a hypothetical case where $|\mathcal{R}_a| = 3$, $r_a = p_2$, and where \tilde{q}_{ar_a} is depicted by the single point.

Recall that variables q_{ap}^\pm become nonzero only when the corresponding resistance p is active (i.e., $x_{ap} = 1$). Also note that, since only one flow direction is chosen per arc in (MICP-R), cuts can be strengthened through multiplication of constants with affine expressions of y_a . Exploiting these properties, aggregating over all $r_a \in \mathcal{R}_a$ and $\tilde{q}_{ar_a}^\pm$ allows the rewriting of Constraints (19) as

$$\tilde{\tau}_{ar_a}^+ y_a + \alpha \sum_{p \in \mathcal{R}_a} p (\tilde{q}_{ap}^+)^{\alpha-1} q_{ap}^+ \leq \frac{\Delta h_a^+}{L_a}, \forall a \in \mathcal{A}, \forall r_a \in \mathcal{R}_a, \forall \tilde{q}_{ar_a}^+ \in \mathcal{Q}_{ar_a}^+ \quad (22a)$$

$$\tilde{\tau}_{ar_a}^- (1 - y_a) + \alpha \sum_{p \in \mathcal{R}_a} p (\tilde{q}_{ap}^-)^{\alpha-1} q_{ap}^- \leq \frac{\Delta h_a^-}{L_a}, \forall a \in \mathcal{A}, \forall r_a \in \mathcal{R}_a, \forall \tilde{q}_{ar_a}^- \in \mathcal{Q}_{ar_a}^-, \quad (22b)$$

where $\tilde{\tau}_{ar_a}^\pm := (1 - \alpha) r_a (\tilde{q}_{ar_a}^\pm)^\alpha$ for brevity, and $\mathcal{Q}_{ar_a}^\pm = [0, \bar{q}_{ar_a}^\pm]$. Raghunathan (2013) shows that each cut of Constraints (22) is, in fact, *stronger* than the set of standard disaggregated cuts that outer-approximate Constraints (19). Also, as shown in Section 4.4, algorithmically, $\mathcal{Q}_{ar_a}^\pm$ can instead be replaced by the finite sets $\tilde{\mathcal{Q}}_{ar_a}^\pm$ to linearly *approximate* (MICP-R) rather than reproduce it.

Feasibility Cutting Planes Since (MICP-R) is a relaxation of (MINLP), a design solution to (MICP-R) is not guaranteed to be physically feasible. To address this, let $\bar{\mathcal{X}}$ denote the set of designs represented by binary vectors \bar{x} satisfying Constraints (11) that are *not* physically feasible. Then, any infeasible designs permitted by (MICP-R) will be excluded by the set of linear cuts

$$\sum_{a \in \mathcal{A}} \left[\left(\sum_{p \in \mathcal{R}_a: \bar{x}_{ap}=1} x_{ap} \right) - \left(\sum_{p \in \mathcal{R}_a: \bar{x}_{ap}=0} x_{ap} \right) \right] \leq |\mathcal{A}| - 1, \forall \bar{x} \in \bar{\mathcal{X}}. \quad (23)$$

Each Constraint (23) is a traditional combinatorial “no good” cut, which removes *one* combination of resistances (i.e., one network design) from the space of solutions feasible to (MICP-R).

Mixed-integer Linear Reformulation Combining much of (MICP-R) with the cuts described in this section, the infinite MIP reformulation of (MINLP), which abstractly describes the theoretical contributions of and foundational formulation used by Raghunathan (2013), is

$$\begin{aligned}
& \text{minimize} && \text{Objective function: } \eta(x) \text{ of Equation (13)} \\
& \text{subject to} && \text{Physical bounds: Constraints (2), (3), (15)} \\
& && \text{Flow conservation: Constraints (4)} \\
& && \text{Resistance selection: Constraints (11)} \tag{MIP-R} \\
& && \text{Head difference relationships: Constraints (16), (20), (22)} \\
& && \text{Direction-related inequalities: Constraints (17)} \\
& && \text{Feasibility cutting planes: Constraints (23)}.
\end{aligned}$$

Algorithmically, the sets $\mathcal{Q}_{ar_a}^\pm$ and $\bar{\mathcal{X}}$ of Constraints (22) and (23) are replaced by the initially empty finite sets, $\tilde{\mathcal{Q}}_{ar_a}^\pm$ and $\tilde{\mathcal{X}}$, and progressively augmented during the algorithm's execution. Hereafter, we refer to the relaxation of (MIP-R) as (MIP-RR). To refine this relaxation, the convex oracle algorithmically used for determining whether a design is contained in $\bar{\mathcal{X}}$ is described in Section 4.3.

4.3. Convex Method for Determining Design Feasibility

This section reviews the work of Cherry (1951) and Raghunathan (2013), who provide a convex program for determining the feasibility of a nonlinear network with fixed resistances r . These resistances correspond to an integer solution \hat{x} satisfying Constraints (11) via the relationship

$$r_a \in \{p \in \mathcal{R}_a : \hat{x}_{ap} = 1\}, \forall a \in \mathcal{A}. \tag{24}$$

Thus, this feasibility-testing method can be used to determine whether \hat{x} is contained in $\bar{\mathcal{X}}$. Letting q_a^\pm denote nonnegative directed flow variables along $a \in \mathcal{A}$ and using the definition $q_a := q_a^+ - q_a^-$, the studies ultimately propose a strictly convex programming problem similar to

$$\begin{aligned}
& \text{minimize}_{q^\pm \geq 0} && \sum_{a \in \mathcal{A}} \frac{L_a r_a}{1 + \alpha} [(q_a^+)^{1+\alpha} + (q_a^-)^{1+\alpha}] - \sum_{i \in \mathcal{S}} h_i^s \sum_{a \in \delta_i^+} q_a \\
& \text{subject to} && \sum_{a \in \delta_i^-} q_a - \sum_{a \in \delta_i^+} q_a = d_i, \forall i \in \mathcal{J}.
\end{aligned} \tag{P(r)}$$

Ragunathan (2013) proves three important properties of $(P(r))$: (i) its solution \hat{q} is unique; (ii) the dual multipliers of flow conservation constraints correspond to unique heads \hat{h} ; and (iii) the primal-dual solution (\hat{q}, \hat{h}) satisfies flow conservation and head loss Constraints (4) and (8). The ability to find a solution (\hat{q}, \hat{h}) satisfying these physical equations by solving $(P(r))$ is appealing because the feasibility of r can be tested by checking whether (\hat{q}, \hat{h}) satisfies Constraints (1) and (3). Ragunathan uses this method to guarantee global convergence of their relaxation-based algorithm.

4.4. Global Optimization Algorithm

This section outlines a simple algorithm for solving (MINLP) to global optimality via the iterative solution and augmentation of (MIP-RR). Algorithm 1 leverages the outer approximation and feasibility cuts established in Section 4.2. In Line 1, the outer approximation point sets and infeasible design set, \tilde{Q}^\pm and $\tilde{\mathcal{X}}$, are initialized as empty. In Line 2, the relaxed problem is solved, and the solution components $(\hat{q}, \hat{h}, \hat{x})$ are stored. In Line 3, feasibility of the design \hat{x} is determined (e.g., via the method of Section 4.3). If the design is found to be physically infeasible, outer approximations of head loss constraints are added in Line 4. A feasibility cut that excludes \hat{x} is then added in Line 5. Finally, a solution to the new relaxed problem, with the aforementioned cuts, is obtained in Line 6. These steps are repeated until a feasible solution \hat{x} to (MINLP) is identified. Since this \hat{x} is discovered via the solution of sequential *relaxations* of (MINLP) and the cuts do not exclude feasible solutions to (MINLP), the design obtained is guaranteed to be globally optimal.

In practice, the algorithm developed by Ragunathan (2013) is more sophisticated than Algorithm 1. Specifically, it exploits the linearization-based linear programming/nonlinear programming branch and bound (LP/NLP-BB) framework developed by Quesada and Grossmann (1992). This permits more flexibility than Algorithm 1 through the use of “callback” features available in many MIP solvers. First, outer approximations are added in other parts of the search tree, not just integer solutions to (MIP-RR), as in Line 4. Moreover, outer approximation points \tilde{Q}^\pm are more thoughtfully selected. Second, Ragunathan develops heuristic procedures, internal to the search, that can recover feasible solutions from fractional solutions and integer solutions *infeasible* to (MINLP).

Algorithm 1 A MIP relaxation-based global optimization algorithm for (MINLP).

- 1: $\tilde{Q}_{ap}^{\pm} \leftarrow \emptyset, \forall a \in \mathcal{A}, \forall p \in \mathcal{R}_a; \tilde{\mathcal{X}} \leftarrow \emptyset.$
 - 2: $(\hat{q}, \hat{h}, \hat{x}) \leftarrow \text{Solve (MIP-RR).}$
 - 3: **while** \hat{x} is infeasible to (MINLP) **do**
 - 4: $\tilde{Q}_{ap}^{\pm} \leftarrow \tilde{Q}_{ap}^{\pm} \cup \{\hat{q}_{ap}^{\pm}\}, \forall a \in \mathcal{A}, \forall p \in \mathcal{R}_a.$
 - 5: $\tilde{\mathcal{X}} \leftarrow \tilde{\mathcal{X}} \cup \{\hat{x}\}.$
 - 6: $(\hat{q}, \hat{h}, \hat{x}) \leftarrow \text{Solve (MIP-RR).}$
 - 7: **end while**
-

In this paper, the majority of Raghunathan’s contributions are used to devise a new algorithm, which is further discussed in Section 6. The two algorithms primarily differ in the selection of outer approximation cuts. To understand our algorithm, Section 5 describes the novel contributions that eventually lead to these new cuts, which are derived and applied in Section 6. Note that a more thorough algorithmic description is presented in Appendix C.

5. Convex Reformulation

Section 4.3 summarizes a convex method for determining the feasibility of a nonlinear network with fixed resistances. This method could be exploited within a bilevel programming formulation for optimal design, whereby resistance selections obtained in the outer level must satisfy constraints on the corresponding solution of $(P(r))$ (i.e., the inner level). Indeed, such a bilevel method was developed by Zhang and Zhu (1996) for the design of pipe networks. Interestingly, however, no study has fully examined nor exploited the relationship between $(P(r))$ and its (strong) dual, which we show leads to exact convex reformulations of the original feasibility and design problems. This section describes two of our novel contributions, both of which serve as foundations for the remainder of this paper. The first subsection derives an *exact* convex reformulation of $(NLP(r))$. The second subsection then extends this result to derive an *exact* MICP reformulation of (MINLP).

5.1. Convex Reformulation of $(NLP(r))$

This section extends Section 4.3 to derive an exact convex reformulation of $(NLP(r))$ based on optimality conditions for $(P(r))$ and the addition of physical bounds. Note that the objective

function of $(P(r))$ is convex and all constraints are affine. The linearity constraint qualification thus implies the existence of a strong dual. This dual problem is thoroughly derived in Appendix A using conventional Lagrangian duality theory. It is expressed here as

$$\begin{aligned}
 & \underset{\Delta h^\pm \geq 0}{\text{maximize}} && \frac{-\alpha}{1+\alpha} \sum_{a \in \mathcal{A}} \frac{1}{\sqrt[\alpha]{L_a r_a}} \left[(\Delta h_a^+)^{1+\frac{1}{\alpha}} + (\Delta h_a^-)^{1+\frac{1}{\alpha}} \right] - \sum_{i \in \mathcal{J}} h_i d_i \\
 & \text{subject to} && \Delta h_a^+ - \Delta h_a^- = h_i^s - h_j, \quad \forall a := (i, j) \in \mathcal{A} : i \in \mathcal{S} \\
 & && \Delta h_a^+ - \Delta h_a^- = h_i - h_j, \quad \forall a := (i, j) \in \mathcal{A} : i \in \mathcal{J}.
 \end{aligned} \tag{D(r)}$$

THEOREM 1. *Let $f_P(q)$ and $f_D(h)$ denote the objective functions of $(P(r))$ and $(D(r))$, respectively, and $q_a := q_a^+ - q_a^-$, $\forall a \in \mathcal{A}$. The following convex problem is equivalent to $(NLP(r))$:*

$$\begin{aligned}
 & f_P(q) - f_D(h) \leq 0 \\
 & \sum_{a \in \delta_i^-} q_a - \sum_{a \in \delta_i^+} q_a = d_i, \quad \forall i \in \mathcal{J} \\
 & \Delta h_a^+ - \Delta h_a^- = h_i^s - h_j, \quad \forall a := (i, j) \in \mathcal{A} : i \in \mathcal{S} \\
 & \Delta h_a^+ - \Delta h_a^- = h_i - h_j, \quad \forall a := (i, j) \in \mathcal{A} : i \in \mathcal{J} \\
 & \underline{h}_i \leq h_i \leq \bar{h}_i, \quad \forall i \in \mathcal{J}, \quad 0 \leq q_a^\pm \leq \bar{q}_a^\pm, \quad \Delta h_a^\pm \geq 0, \quad \forall a \in \mathcal{A}.
 \end{aligned} \tag{CP(r)}$$

Proof of Theorem 1 By weak duality, it follows that $f_P(q) \geq f_D(h)$ for any feasible solutions to $(P(r))$ and $(D(r))$, with equality holding for optimal solutions by strong duality. As a result, optimality is equivalently imposed by combining constraints of $(P(r))$ and $(D(r))$ with the *convex* constraint $f_P(q) - f_D(h) \leq 0$. Next, Raghunathan (2013) shows that head loss Constraints (8) of $(NLP(r))$ are equivalent to a portion of the first order optimality conditions for $(P(r))$. Moreover, Section 5.5.3 of Boyd and Vandenberghe (2004) ensures that, since $(P(r))$ is a convex differentiable problem with a strong dual, the dual multipliers h appearing in its optimality conditions are optimal solutions of the dual problem $(D(r))$. That is, any (q, h) that satisfies the constraints of $(P(r))$ and $(D(r))$ and strong duality will also satisfy flow conservation and head loss Constraints (4) and (8). Finally, appending bound constraints on q and h ensures equivalence to $(NLP(r))$. \square

A physical interpretation of the convex strong duality constraint is discussed in Appendix B. Summarily, the constraint implies the conservation of power, with an inequality replacing the traditional equality. Nonetheless, it is known via the strong duality argument above that any solution to (CP(r)) will indeed satisfy this constraint with equality.

5.2. Mixed-integer Convex Reformulation of (MINLP)

To reformulate (MINLP) using (CP(r)), we first introduce continuous flow variables q_{ap}^\pm as in Equations (14), and binary resistance selection variables x_{ap} , subject to bound Constraints (15). Next, we introduce continuous variables Δh_{ap}^\pm and derive their bounds from Constraints (3), i.e.,

$$0 \leq \Delta h_{ap}^\pm \leq \Delta \bar{h}_{ap}^\pm x_{ap}, \quad x_{ap} \in \mathbb{B}, \quad \forall a \in \mathcal{A}, \quad \forall p \in \mathcal{R}_a. \quad (25)$$

The constraints involving head differences in (CP(r)) are next rewritten as

$$\sum_{p \in \mathcal{R}_a} (\Delta h_{ap}^+ - \Delta h_{ap}^-) = h_i - h_j, \quad \forall a := (i, j) \in \mathcal{A} : i \in \mathcal{J} \quad (26a)$$

$$\sum_{p \in \mathcal{R}_a} (\Delta h_{ap}^+ - \Delta h_{ap}^-) = h_i^s - h_j, \quad \forall a := (i, j) \in \mathcal{A} : i \in \mathcal{S}. \quad (26b)$$

Finally, the strong duality constraint appearing in (CP(r)) is expanded over all $p \in \mathcal{R}_a$ as

$$\begin{aligned} & \frac{1}{1+\alpha} \sum_{a \in \mathcal{A}} L_a \sum_{p \in \mathcal{R}_a} p [(q_{ap}^+)^{1+\alpha} + (q_{ap}^-)^{1+\alpha}] - \sum_{i \in \mathcal{S}} h_i^s \sum_{a \in \delta_i^+} q_a \\ & + \frac{\alpha}{1+\alpha} \sum_{a \in \mathcal{A}} \sum_{p \in \mathcal{R}_a} \frac{1}{\sqrt[\alpha]{L_a p}} [(\Delta h_{ap}^+)^{1+\frac{1}{\alpha}} + (\Delta h_{ap}^-)^{1+\frac{1}{\alpha}}] + \sum_{i \in \mathcal{J}} h_i d_i \leq 0. \end{aligned} \quad (27)$$

These expansions of (CP(r)) give rise to the *exact* mixed-integer convex reformulation of (MINLP), where Constraints (4) employ the definitions of q_a described in Equations (14). Namely,

minimize Objective function: $\eta(x)$ of Equation (13)

subject to Physical bounds: Constraints (3), (15), (25)

Flow conservation: Constraints (4)

(MICP-E)

Resistance selection: Constraints (11)

Head difference equalities: Constraints (26)

Strong duality: Constraint (27).

THEOREM 2. *A design \hat{x} is feasible for (MICP-E) if and only if it is feasible for (MINLP).*

Proof of Theorem 2 For any binary \hat{x} satisfying Constraints (11), (MINLP) reduces to (NLP(r)) and (MICP-E) to (CP(r)), with r given by Equations (24). For any r , (NLP(r)) and (CP(r)) are equivalent by Theorem 1. Thus, the sets of feasible \hat{x} for (MINLP) and (MICP-E) are equal. \square

Constraint (27) of (MICP-E) can be viewed as a convex embedding of Constraints (12). Although convexity is desirable, Constraint (27) is highly aggregated. In this sense, the disaggregated nonconvex Constraints (12) of (MINLP) or convex Constraints (19) of (MICP-R) may be more numerically useful. Section 6 uses this observation to construct a relaxation-based global algorithm based on (MICP-E) and (MICP-R) that outer-approximates Constraint (27) and Constraints (19).

6. Novel Cutting Planes and Algorithmic Enhancements

As discussed in Section 5.2, (MICP-E) is an exact reformulation of the design problem. As such, it can be posed directly to an MICP solver (e.g., BONMIN, Bonami et al. 2008) to obtain a globally optimal solution. In practice, however, direct methods converge slowly, as modern MICP solvers do not efficiently handle nonquadratic nonlinear relationships (e.g., Constraint (27)). On the other hand, modern MIP solvers are highly efficient but require conscientious linearizations of (MICP-E). This section pursues the latter, following a structure similar to Section 4. Specifically, it introduces novel outer approximation cuts while developing a MIP reformulation and relaxation of (MICP-E), then summarizes this paper's extensions to the algorithm of Raghunathan (2013).

Flow Direction-based Inequalities Although (MICP-E) does not require flow direction variables y_a , we nonetheless incorporate y_a to strengthen inequalities throughout our linearized reformulation. Similar to Constraints (17), flows and head differences are bounded via

$$0 \leq q_{ap}^+ \leq \bar{q}_{ap}^+ y_a, \quad 0 \leq q_{ap}^- \leq \bar{q}_{ap}^- (1 - y_a), \quad y_a \in \mathbb{B}, \quad \forall a \in \mathcal{A}, \quad \forall p \in \mathcal{R}_a \quad (28a)$$

$$0 \leq \Delta h_{ap}^+ \leq \bar{\Delta h}_{ap}^+ y_a, \quad 0 \leq \Delta h_{ap}^- \leq \bar{\Delta h}_{ap}^- (1 - y_a), \quad y_a \in \mathbb{B}, \quad \forall a \in \mathcal{A}, \quad \forall p \in \mathcal{R}_a. \quad (28b)$$

We also employ valid inequalities to exploit a priori knowledge concerning flow directionality throughout the network. The inequalities proposed here are similar to those described by

Borraz-Sánchez et al. (2016) in the context of natural gas network expansion planning. The first are

$$\sum_{a \in \delta_i^+} y_a \geq 1, \quad \forall i \in \mathcal{S}, \quad (29)$$

which model that at least one pipe must send water *away* from each source. The next are

$$\sum_{a \in \delta_i^-} y_a + \sum_{a \in \delta_i^+} (1 - y_a) \geq 1, \quad i \in \mathcal{J} : d_i > 0, \quad (30)$$

which model that at least one pipe must provide water *to* each demand node. Finally,

$$\sum_{a \in \delta_i^-} y_a - \sum_{a \in \delta_i^+} y_a = 0, \quad i \in \mathcal{J} : (d_i = 0) \wedge (\deg_i^+ = \deg_i^- = 1) \quad (31a)$$

$$\sum_{a \in \delta_i^-} y_a + \sum_{a \in \delta_i^+} y_a = 1, \quad i \in \mathcal{J} : (d_i = 0) \wedge (\deg_i^\pm = 2) \wedge (\deg_i^\mp = 0) \quad (31b)$$

are constraints that model flow directionality at junctions with zero demand and degree two, with the implication that the direction of incoming flow must be equal to the direction of outgoing flow.

Head Loss Outer Approximation Cutting Planes Although also not required by (MICP-E), head loss relationships are used to further strengthen linearization-based reformulations. Similar to Constraints (22) in (MIP-R), we express these head loss outer approximations as

$$\tilde{\tau}_{ar_a}^+ y_a + \alpha \sum_{p \in \mathcal{R}_a} p (\tilde{q}_{ap}^+)^{\alpha-1} q_{ap}^+ \leq \sum_{p \in \mathcal{R}_a} \frac{\Delta h_{ap}^+}{L_a}, \quad \forall a \in \mathcal{A}, \forall r_a \in \mathcal{R}_a, \forall \tilde{q}_{ar_a}^+ \in \mathcal{Q}_{ar_a}^+ \quad (32a)$$

$$\tilde{\tau}_{ar_a}^- (1 - y_a) + \alpha \sum_{p \in \mathcal{R}_a} p (\tilde{q}_{ap}^-)^{\alpha-1} q_{ap}^- \leq \sum_{p \in \mathcal{R}_a} \frac{\Delta h_{ap}^-}{L_a}, \quad \forall a \in \mathcal{A}, \forall r_a \in \mathcal{R}_a, \forall \tilde{q}_{ar_a}^- \in \mathcal{Q}_{ar_a}^- \quad (32b)$$

Furthermore, similar to Constraints (19), we linearly upper-bound each head difference with

$$\Delta h_{ap}^\pm \leq L_a p (\bar{q}_{ap}^\pm)^{\alpha-1} q_{ap}^\pm, \quad \forall a \in \mathcal{A}, \forall p \in \mathcal{R}_a. \quad (33)$$

Strong Duality Cutting Planes A primary contribution of this paper is the strong duality Constraint (27) of (MICP-E). To linearize this constraint, we define variables $q_a^{\text{NL}}, \Delta h_a^{\text{NL}} \geq 0$ to approximate the sums of nonlinear terms involving q_{ap}^\pm and Δh_{ap}^\pm in the original constraint, i.e.,

$$q_a^{\text{NL}} = \frac{1}{1 + \alpha} \sum_{p \in \mathcal{R}_a} p \left[(q_{ap}^+)^{1+\alpha} + (q_{ap}^-)^{1+\alpha} \right], \quad \forall a \in \mathcal{A} \quad (34a)$$

$$\Delta h_a^{\text{NL}} = \frac{\alpha}{1 + \alpha} \sum_{p \in \mathcal{R}_a} \frac{1}{\sqrt[p]{p}} \left[(\Delta h_{ap}^+)^{1+\frac{1}{\alpha}} + (\Delta h_{ap}^-)^{1+\frac{1}{\alpha}} \right], \quad \forall a \in \mathcal{A}. \quad (34b)$$

This permits a purely linear rewriting of the original strong duality constraint, namely

$$\sum_{a \in \mathcal{A}} L_a q_a^{\text{NL}} - \sum_{i \in \mathcal{S}} h_i^s \sum_{a \in \delta_i^+} \sum_{p \in \mathcal{R}_a} (q_{ap}^+ - q_{ap}^-) + \sum_{a \in \mathcal{A}} \frac{\Delta h_a^{\text{NL}}}{\sqrt[\alpha]{L_a}} + \sum_{i \in \mathcal{J}} h_i d_i \leq 0. \quad (35)$$

Observe that the right-hand sides of Equations (34) are convex. Similar to the head loss outer approximations derived in Section 4.2, we follow the notion of *equal intercept* linear outer approximations to compose cuts similar to Constraints (32) for q_a^{NL} and Δh_a^{NL} . For q_a^{NL} , let the intercept be determined by the linear approximation to the term corresponding to $r_a \in \mathcal{R}_a$ at point $\tilde{q}_{ar_a}^\pm$. For each remaining $p \in \mathcal{R}_a$, the same intercept is achieved by the linear approximation at point $\tilde{q}_{ap}^\pm := \tilde{q}_{ar_a}^\pm (r_a/p)^{1/(1+\alpha)}$. With these values in mind, the outer approximations are then

$$\tilde{\zeta}_{ar_a}^+ y_a + \sum_{p \in \mathcal{R}_a} p (\tilde{q}_{ap}^+)^{\alpha} q_{ap}^+ \leq q_a^{\text{NL}}, \forall a \in \mathcal{A}, \forall r_a \in \mathcal{R}_a, \forall \tilde{q}_{ar_a}^+ \in \mathcal{Q}_{ar_a}^{\text{NL}^+} \quad (36a)$$

$$\tilde{\zeta}_{ar_a}^- (1 - y_a) + \sum_{p \in \mathcal{R}_a} p (\tilde{q}_{ap}^-)^{\alpha} q_{ap}^- \leq q_a^{\text{NL}}, \forall a \in \mathcal{A}, \forall r_a \in \mathcal{R}_a, \forall \tilde{q}_{ar_a}^- \in \mathcal{Q}_{ar_a}^{\text{NL}^-}, \quad (36b)$$

where $\mathcal{Q}_{ar_a}^{\text{NL}^\pm} = [0, \tilde{q}_{ar_a}^\pm]$, and $\tilde{\zeta}_{ar_a}^\pm := \left(\frac{1}{1+\alpha} - 1\right) r_a (\tilde{q}_{ar_a}^\pm)^{1+\alpha}$ is defined for notational brevity.

An analogous procedure is followed for Δh_a^{NL} . Similar to Constraints (36), assuming $\Delta \tilde{h}_{ap}^\pm$ are points with coinciding outer approximation intercepts, the aggregated outer approximations are

$$-\xi_{ar_a}^\pm y_a + \sum_{p \in \mathcal{R}_a} \left(\sqrt[\alpha]{\frac{\Delta \tilde{h}_{ap}^+}{p}} \right) \Delta h_{ap}^+ \leq \Delta h_a^{\text{NL}}, \forall a \in \mathcal{A}, \forall r_a \in \mathcal{R}_a, \forall \Delta \tilde{h}_{ar_a}^+ \in \mathcal{H}_{ar_a}^{\text{NL}^+} \quad (37a)$$

$$-\xi_{ar_a}^\pm (1 - y_a) + \sum_{p \in \mathcal{R}_a} \left(\sqrt[\alpha]{\frac{\Delta \tilde{h}_{ap}^-}{p}} \right) \Delta h_{ap}^- \leq \Delta h_a^{\text{NL}}, \forall a \in \mathcal{A}, \forall r_a \in \mathcal{R}_a, \forall \Delta \tilde{h}_{ar_a}^- \in \mathcal{H}_{ar_a}^{\text{NL}^-}, \quad (37b)$$

where $\mathcal{H}_{ar_a}^{\text{NL}^\pm} = [0, \Delta \tilde{h}_{ar_a}^\pm]$, and $\xi_{ar_a}^\pm := \frac{(\Delta \tilde{h}_{ar_a}^\pm)^{1+\frac{1}{\alpha}}}{(1+\alpha) \sqrt[\alpha]{r_a}}$ is similarly defined for notational brevity.

Mixed-integer Linear Reformulation With the variables and constraints previously described, a MIP reformulation of (MICP-E) may be written in a manner similar to (MIP-R), that is,

$$\begin{aligned}
 &\text{minimize} && \text{Objective function: } \eta(x) \text{ of Equation (13)} \\
 &\text{subject to} && \text{Physical bounds: Constraints (3), (15), (25)} \\
 &&& \text{Flow conservation: Constraints (4)} \\
 &&& \text{Resistance selection: Constraints (11)} \\
 &&& \text{Head difference relationships: Constraints (26), (32), (33)} \\
 &&& \text{Direction-related inequalities: Constraints (28)–(31)} \\
 &&& \text{Strong duality: Constraints (36), (37)} \\
 &&& \text{Feasibility cutting planes: Constraints (23)}.
 \end{aligned}
 \tag{MIP-E}$$

Similarly to (MIP-R), algorithmically, the sets \mathcal{Q}^\pm , $\mathcal{Q}^{\text{NL}\pm}$, $\mathcal{H}^{\text{NL}\pm}$, and $\tilde{\mathcal{X}}$ of Constraints (32), (36), (37), and (23) are instead replaced by the initially empty finite sets $\tilde{\mathcal{Q}}^\pm$, $\tilde{\mathcal{Q}}^{\text{NL}\pm}$, $\tilde{\mathcal{H}}^{\text{NL}\pm}$, and $\tilde{\mathcal{X}}$, respectively. These changes give rise to the further (finite) linear relaxation, named (MIP-ER).

Algorithmic Enhancements Our algorithm, which is omitted here for brevity but exploits (MIP-ER), is similar to that of Raghunathan (2013) but differs in a few important respects. Primarily, Raghunathan only applies outer approximations similar to Constraints (32), which correspond to convexified head loss relationships. Our algorithm extends this by adding outer approximations of terms appearing in the strong duality Constraint (27). A more thorough comparison and presentation of the two algorithms is presented in Appendix C.

7. Computational Experiments

This section compares the convergence of our new algorithm and an algorithm based on Raghunathan (2013). Both were implemented in the JULIA programming language using JUMP, version 0.20 (Dunning et al. 2017), and version 0.1 of WATERMODELS, an open-source JULIA package for water distribution network optimization (Tasseff et al. 2019a). Section 7.1 describes the instances, computational resources, and parameters used in the experiments; Section 7.2 compares

Network	# Nodes	# Arcs	# Resistances	# Binary Variables	# Designs
shamir	8	8	14	120	1.48×10^9
blacksburg	32	23	14	369	2.30×10^{26}
hanoi	33	34	6	238	2.87×10^{26}
foss_poly_0	38	58	7	464	1.04×10^{49}
foss_iron	38	58	13	812	4.06×10^{64}
foss_poly_1	38	58	22	1334	7.25×10^{77}
pescara	74	99	13	1386	1.91×10^{110}
modena	276	317	13	4438	1.32×10^{353}

Table 1 Summary of benchmark instances from the literature and their combinatorial sizes. Here, “# Arcs” is the number of arcs with $|\mathcal{R}_a| \neq 1$; “# Resistances” is $|\mathcal{R}_a|$ per variable pipe; “# Binary Variables” is $|x| + |y|$ for MIP formulations; and “# Designs” is the total number of unique designs satisfying Constraints (11).

the efficacy of the two algorithms by examining convergence; and Section 7.3 compares their performance on an extended set of instances obtained by scaling demand across all junctions.

7.1. Experimental Setup

The numerical experiments consider instances of varying sizes that appear in the water network design literature and are summarized in Table 1 (D’Ambrosio et al. 2015, Mala-Jetmarova et al. 2018). All use the Hazen-Williams head loss relationship originally defined by Equation (7). The set of *diameters* in each problem gives a set of *resistances*, each being proportional to $D_{ap}^{-4.8704}$.

The instances of Table 1 are divided into two classes: *moderate* instances, comprising *shamir*, *blacksburg*, *hanoi*, *foss_poly_0*, and *foss_iron*; and *large* instances, comprising *foss_poly_1*, *pescara*, and *modena*. Generally, moderate instances are solvable to optimality with both algorithms given a sufficient amount of time (i.e., seconds to hours), while large instances cannot be solved, even given substantial time (i.e., days). Each experiment began each algorithm with equivalent data, initial feasible solutions, and outer approximation points. Parameters of the two algorithms were chosen to coincide with those used by Raghunathan and are detailed in Appendix D.

Experiments were performed on Los Alamos National Laboratory’s Darwin computing cluster. Each was executed on a node containing two Intel Xeon E5-2695 v4 processors, each with 18 cores @2.10 GHz, and 125 GB of memory. Excluding the small amount of time required by Raghunathan’s heuristic procedure to obtain an initial feasible solution (seconds), each experiment was provided

a wall-clock time of 171,900 seconds (approximately two days). For solutions of the MIPs, GUROBI 9.0.3 was used with `Cuts=0`, which disables all of GUROBI’s internal cutting plane methods. For moderate instances, `Heuristics=0.0` was used, which disables GUROBI’s internal heuristics. For large instances, `MIPFocus=1` was used, which places a focus on finding feasible solutions quickly.

For convex subproblems, e.g., the solution of $(P(r))$, IPOPT version 3.13 was used (Wächter and Biegler 2006). As per Tasseff et al. (2019b), since these problems are small, the linear solver MA57 was employed. The settings `warm_start_init_point="yes"` and `nlp_scaling_method="none"` were also used. Heuristically, these parameters computed solutions to $(P(r))$ most efficiently.

7.2. Comparison of Algorithms on Standard Benchmark Instances

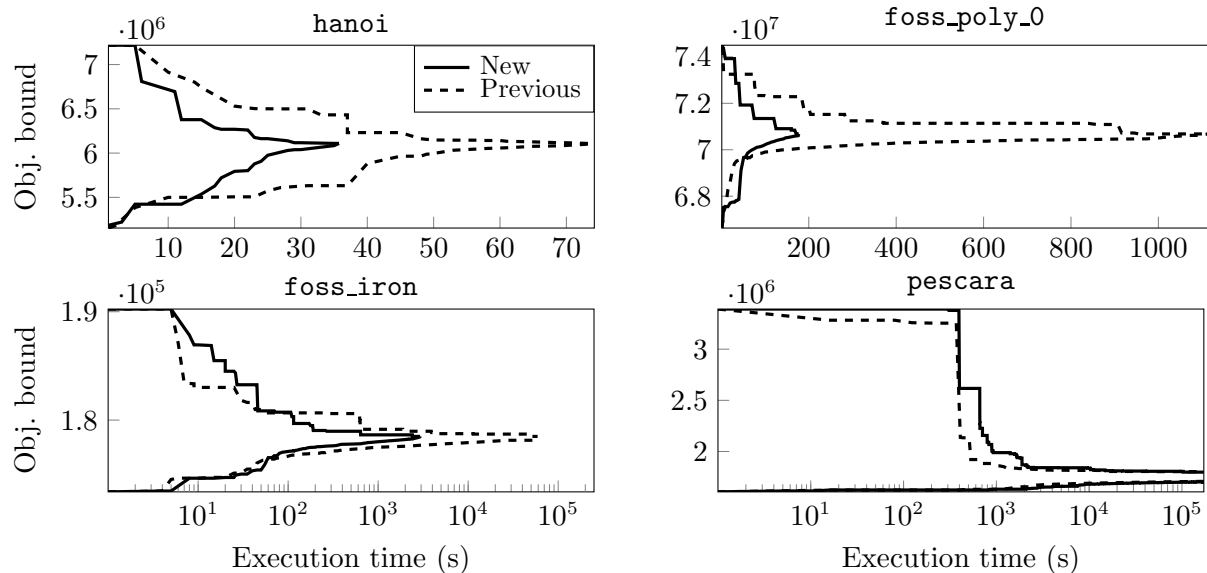


Figure 2 Convergence of objective bounds on select instances, comparing the new algorithm with an algorithm similar to Raghunathan (2013) (Previous). Note the use of linear and logarithmic abscissas.

Figure 2 illustrates the lower and upper bound convergence of the two algorithms on a representative subset of instances (i.e., `hanoi`, `foss_poly_0`, `foss_iron`, and `pescara`). Here, both algorithms converge to global optimality on the three moderate instances, with the new algorithm displaying more favorable performance, i.e., lower and upper bounds converging more quickly. However,

Problem	Previous Algorithm			New Algorithm		
	Gap (%)	Nodes Expl.	Time (s)	Gap (%)	Nodes Expl.	Time (s)
shamir	0.00	12,098	12.27	0.00	2,567	7.11
hanoi	0.00	32,024	74.21	0.00	24,765	35.74
blacksburg	0.00	16,009	14.05	0.00	15,971	29.25
foss_poly_0	0.00	144,226	1,112.78	0.00	63,120	177.08
foss_iron	0.00	1,307,123	59,088.98	0.00	282,202	2,923.24
foss_poly_1	4.19	48,320,343	Limit	4.90	21,858,635	Limit
pescara	5.26	5,633,461	Limit	5.29	2,010,998	Limit
modena	33.77	329,614	Limit	41.65	55,592	Limit

Table 2 Comparison of optimality gaps, nodes explored, and solution times for the new algorithm and one similar to Raghunathan (2013) (Previous). Bold denotes better (smaller) times, nodes explored, and gaps.

Problem	Solutions from the Literature		Solutions from This Study	
	Lower Bnd.	Upper Bnd.	Lower Bnd.	Upper Bnd.
shamir	419,000 ^{1*}	419,000 ^{1*}	419,000 *	419,000 *
hanoi	6,109,620.09 ^{1*}	6,109,620.09 ^{1*}	6,109,620.90 *	6,109,620.90 *
blacksburg	118,251.09 ^{1*}	118,251.09 ^{1*}	118,251.09 *	118,251.09 *
foss_poly_0	70,063,161.90 ¹	70,680,507.90 ²	70,680,507.90 *	70,680,507.90 *
foss_iron	177,512.42 ¹	178,494.14 ¹	178,494.14 *	178,494.14 *
foss_poly_1	26,240.84 ¹	29,202.99 ²	27,269.65	28,462.34
pescara	1,700,517.06 ¹	\approx 1,790,000 ³	1,708,090.52	1,798,252.52
modena	2,206,914.89 ¹	\approx 2,560,000 ⁴	2,198,756.06	3,319,652.71

Table 3 Comparison of best lower and upper bounds from the literature and this study, with bold denoting best bounds, asterisks denoting proven optimality, and blue denoting instances closed for the first time.

References from the literature are labeled as ¹(Raghunathan 2013), ²(Bragalli et al. 2012), ³(Zheng et al. 2017), and ⁴(Artina et al. 2012).

both algorithms can solve `hanoi` in relatively short amounts of times, taking just over a minute to reach global optimality in the worst case. For larger moderate instances (i.e., `foss_poly_0` and `foss_iron`), the differences in convergence behavior are more dramatic. In the case of `foss_poly_0`, the new algorithm converges nearly an order of magnitude more quickly. For `foss_iron`, the difference is further emphasized, with the new algorithm converging more than an order of magnitude faster. *To highlight this point, throughout the literature, neither of these two `foss` instances appear to have been solved to global optimality. Here, both algorithms solve both problems, but ours does so around an order of magnitude faster.* In large cases (e.g., `pescara`), the algorithm of Raghunathan (2013) converges more quickly. This could be for many reasons, the most likely being the more frequent addition of outer approximations in the new algorithm, creating larger BB linear subproblems.

Table 2 provides relevant convergence data for the instances. This table further supports the trends exemplified by Figure 2. For moderate instances, the new algorithm explores fewer nodes to reach optimality. In most of these cases, this node reduction translates to smaller execution times, except for the case of `blacksburg`. For large instances, node exploration appears important for finding new feasible solutions. Thus, the dramatic reduction in the number of nodes explored by the new algorithm has a negative impact on the optimality gap reached by the time limit. Generally, the new algorithm appears useful for instances where optimality can be proven quickly but tends to suffer on large instances because of the increased master problem size — a topic of future work.

Table 3 compares the results from the water network design literature with the best results obtained in this study, including where our implementation of Raghunathan (2013) outperformed the new algorithm. Specifically, the best objective lower and upper bounds are compared. The table depicts many new bounds discovered using the algorithms herein, especially on outstanding instances. (For the three *large* cases, our implementation of Raghunathan’s algorithm, not the new algorithm, discovered the bounds shown. The exception is for our upper bound on `pescara`, which the new algorithm discovered.) Note that here, literature solutions are not differentiated between those obtained heuristically and those obtained via algorithms that can provide lower bounds (e.g., Raghunathan’s algorithm). The slight change in the optimal solution of `hanoi` could be a typographical error of Raghunathan (2013) or a small difference in our definition of resistance.

7.3. Comparison of Algorithms on Instances with Scaled Demands

This section compares the efficacy of the two algorithms on a set of moderate instances extending those described in Section 7.1. For each junction in each network, the original demand was scaled by a factor between 0.5 and 1.5 in steps of 0.05, generating 21 instances per network and producing 105 instances. For `hanoi`, instances with scalings greater than one were infeasible, reducing the final set to 95 instances. For each instance, the time required to prove optimality was measured.

Figure 3 compares the times required to reach optimality across demand-scaled versions of `foss_poly_0` and `foss_iron`. These instances display the most dramatic differences between the

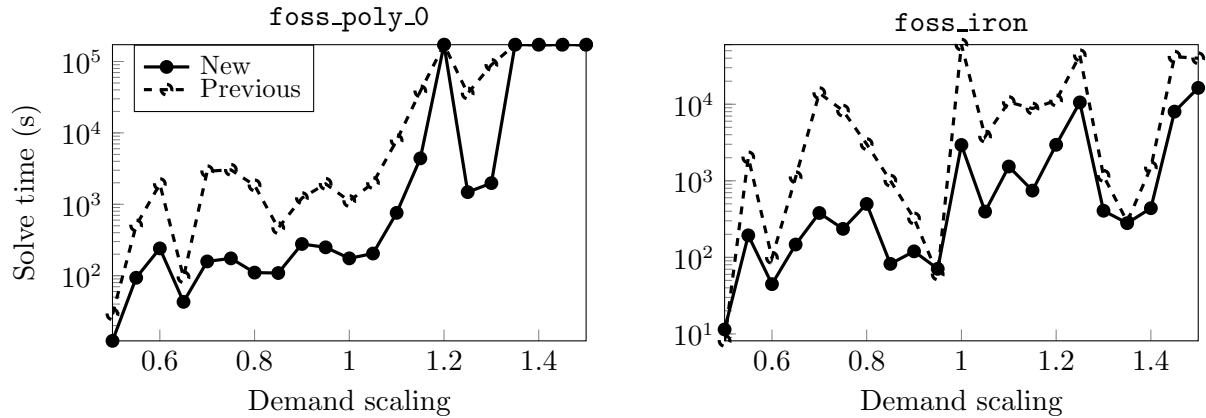


Figure 3 Time (log scale) to reach optimality (if attained) across demand scaling instances for `foss_poly_0` and `foss_iron`, comparing our new algorithm (New) with an algorithm similar to Raghunathan (2013) (Previous).

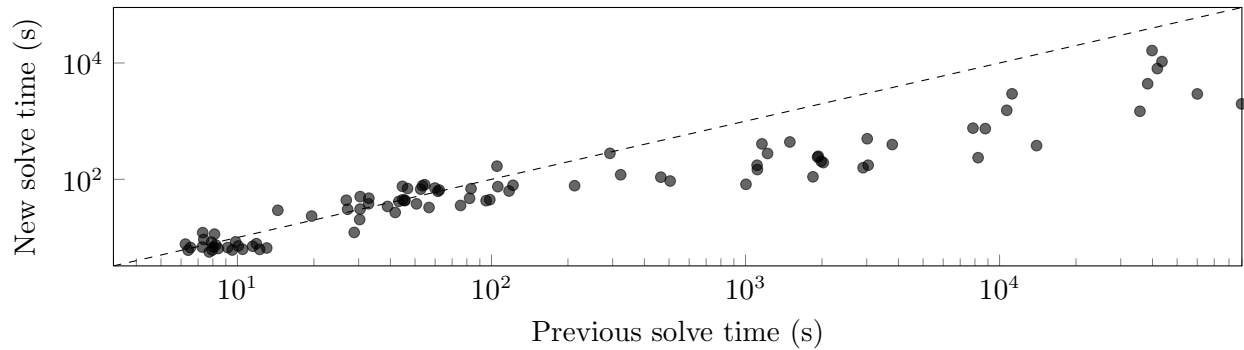


Figure 4 Time (log scale) to solve demand scaling instances with our new algorithm versus an algorithm similar to Raghunathan (2013) (Previous). Instances where optimality was not proven by either are excluded.

two algorithms. For the `foss_poly_0` network, the new algorithm always outperforms the previous algorithm, occasionally by over an order of magnitude. For demand scalings in the set $\{1.2, 1.35, 1.4, 1.45, 1.5\}$, neither algorithm can solve the design instances within the nearly two day time limit. The comparison of solve times in the `foss_iron` plot implies similar behavior. For all instances except two (0.5 and 0.95), the new algorithm outperforms the previous algorithm. Moreover, the new algorithm occasionally outperforms the previous by nearly two orders of magnitude.

Figure 4 compares the times to reach optimality across all demand-scaled instances. The figure excludes the five instances where optimality could not be proven. For instances requiring roughly one hundred seconds or less to reach optimality, the times required by both algorithms are similar, as shown by their placement around the dashed identity line. For instances requiring roughly one

hundred seconds or more, however, the new algorithm always outperforms the previous algorithm, often by one or two orders of magnitude. This supports Section 7.2: for challenging problems where optimality can be proven, our new algorithm outperforms the previous algorithm’s implementation.

8. Concluding Remarks

This study presented the derivation and algorithmic application of a novel, *exact* MICP formulation for the global optimization of potable water distribution network design. Construction of this problem began with a convex reformulation for network design feasibility and extended the models described by Cherry (1951) and Raghunathan (2013) using nonlinear duality. Then, using the new MICP formulation as a foundation, the global, linear relaxation-based algorithm of Raghunathan (2013) was augmented to employ novel outer approximation cuts derived from the new formulation.

To measure its efficacy, our global optimization method was compared against the previous state of the art on standard design instances. Then, new moderately-sized instances were generated by scaling demands throughout the original networks. The combination of results implies significant speedups in convergence (i.e., one to two orders of magnitude) can be achieved on moderately-sized instances for which optimality can be proven within a modest amount of time (i.e., hours).

This study provides a number of novel and useful contributions to the field of water system design and, more broadly, nonlinear network optimization. First and foremost, the formulation of a purely *convex* program for determining design feasibility with the inclusion of physical bounds appears to be the first in the literature. Second and perhaps just as importantly, the exact MICP reformulation of the network design problem establishes a new paradigm for approaching problems of this type. Third, an algorithm based on the novel features of this MICP is presented and appears capable of efficiently proving global optimality on several challenging instances. In fact, our computational results close the optimality gap on two outstanding instances (`foss_poly_0` and `foss_iron`).

Future work will focus on extending the approaches developed herein. First, the convex and mixed-integer convex reformulations appear to be immediately applicable to other application areas, including natural gas network expansion planning and crude oil network optimization. It is

also likely that operational problems for nonlinear networks (e.g., pump scheduling optimization in water networks) can be reformulated exactly using methods similar to those developed herein. Such reformulations may have even greater benefits when considered in these new problem contexts.

Acknowledgments

The authors thank Carleton Coffrin and Kaarthik Sundar of Los Alamos National Laboratory for their expertise in infrastructure optimization and JUMP software development. This work was conducted under the auspices of the National Nuclear Security Administration of the U.S. Department of Energy at Los Alamos National Laboratory under Contract No. 89233218CNA000001. Specifically, work at Los Alamos National Laboratory was supported by the Laboratory Directed Research and Development program under the project *Adaptation Science for Complex Natural-engineered Systems* (20180033DR).

Author Biographies

Byron Tasseff is a scientist at Los Alamos National Laboratory (LANL) in the Information Systems and Modeling group. He earned his M.S. in Industrial and Operations Engineering from the University of Michigan in 2018, where he is also a current Ph.D. candidate. His research involves developing optimization techniques for problems involving fluids and critical infrastructure.

Russell Bent is a scientist at LANL in the Applied Mathematics and Plasma Physics group. He is the principal or co-principal investigator for DOE projects in these areas, with focuses on improving robustness of power systems, increasing resilience of infrastructure networks, modeling interdependencies between systems, managing disasters that impact critical infrastructure, modeling smart grid and microgrid technologies, and developing methods for stochastic optimization.

Marina A. Epelman received her Ph.D. in Operations Research from Massachusetts Institute of Technology. She is currently a professor of Industrial and Operations Engineering at the University of Michigan, with research interests ranging from optimization theory to applications in healthcare and scheduling, among others.

Donatella Pasqualini is a scientist at LANL in the Information Systems and Modeling group. She obtained a Ph.D. in Physics from the University of Trento, Italy. Her research focuses on the co-evolution of natural and critical infrastructure systems under climatic changes.

Pascal Van Hentenryck is the A. Russell Chandler III Chair and Professor in Industrial and Systems Engineering at the Georgia Institute of Technology, as well as the Associate Chair for Innovation and Entrepreneurship. His current research primarily focuses on large-scale optimization and machine learning applied to energy systems and mobility.

Story This work began as part of a LANL project to develop better climate adaptation strategies for critical infrastructure. Early work focused on applying techniques from natural gas network optimization to water network design. After discovering the convex feasibility-testing method of Raghunathan (2013), work shifted toward developing novel feasibility cuts for this problem. Pursuing this further ultimately illuminated a subtle property based on duality, which naturally led to the reformulations presented herein. These reformulations are the first of their kind and have potential applications to other important network problems constrained by nonconvex relationships.

References

- Artina S, Bragalli C, Erbacci G, Marchi A, Rivi M (2012) Contribution of parallel NSGA-II in optimal design of water distribution networks. *Journal of Hydroinformatics* 14(2):310–323.
- Bonami P, Biegler LT, Conn AR, Cornuéjols G, Grossmann IE, Laird CD, Lee J, Lodi A, Margot F, Sawaya N, et al. (2008) An algorithmic framework for convex mixed integer nonlinear programs. *Discrete Optimization* 5(2):186–204.
- Borraz-Sánchez C, Bent R, Backhaus S, Hijazi H, Van Hentenryck P (2016) Convex relaxations for gas expansion planning. *INFORMS Journal on Computing* 28(4):645–656.
- Boyd SP, Vandenberghe L (2004) *Convex Optimization* (Cambridge University Press).
- Bragalli C, D’Ambrosio C, Lee J, Lodi A, Toth P (2012) On the optimal design of water distribution networks: a practical MINLP approach. *Optimization and Engineering* 13(2):219–246.
- Cherry C (1951) CXVII: Some general theorems for non-linear systems possessing reactance. *The London, Edinburgh, and Dublin Philosophical Magazine and Journal of Science* 42(333):1161–1177.
- D’Ambrosio C, Lodi A, Wiese S, Bragalli C (2015) Mathematical programming techniques in water network optimization. *European Journal of Operational Research* 243(3):774–788.

- De Wolf D, Smeers Y (1994) Mathematical properties of formulations of the gas transmission problem. Technical report, SMG Preprint 94/12, Universit libre de Bruxelles.
- Dunning I, Huchette J, Lubin M (2017) JuMP: A modeling language for mathematical optimization. *SIAM Review* 59(2):295–320.
- Gleixner AM, Held H, Huang W, Vigerske S (2012) Towards globally optimal operation of water supply networks. Technical report, Zuse Institute Berlin.
- Humpola J, Fügenschuh A (2013) A new class of valid inequalities for nonlinear network design problems .
- Humpola J, Fügenschuh A, Koch T (2016) Valid inequalities for the topology optimization problem in gas network design. *OR Spectrum* 38(3):597–631.
- Maier H, Kapelan Z, Kasprzyk J, Matott L (2015) Thematic issue on evolutionary algorithms in water resources. *Environmental Modelling & Software* 69:222–225, ISSN 1364-8152, URL <http://dx.doi.org/10.1016/j.envsoft.2015.05.003>.
- Mala-Jetmarova H, Sultanova N, Savic D (2017) Lost in optimisation of water distribution systems? A literature review of system operation. *Environmental Modelling & Software* 93:209–254.
- Mala-Jetmarova H, Sultanova N, Savic D (2018) Lost in optimisation of water distribution systems? A literature review of system design. *Water* 10(3):307.
- Quesada I, Grossmann IE (1992) An LP/NLP based branch and bound algorithm for convex minlp optimization problems. *Computers & Chemical Engineering* 16(10-11):937–947.
- Ragunathan AU (2013) Global optimization of nonlinear network design. *SIAM Journal on Optimization* 23(1):268–295, URL <http://dx.doi.org/10.1137/110827387>.
- Ríos-Mercado RZ, Borraz-Sánchez C (2015) Optimization problems in natural gas transportation systems: A state-of-the-art review. *Applied Energy* 147:536–555, URL <http://dx.doi.org/10.1016/j.apenergy.2015.03.017>.
- Sahebi H, Nickel S, Ashayeri J (2014) Strategic and tactical mathematical programming models within the crude oil supply chain context: A review. *Computers & Chemical Engineering* 68:56–77, URL <http://dx.doi.org/10.1016/j.compchemeng.2014.05.008>.

- Tasseff B, Bent R, Coffrin C (2019a) WaterModels.jl. <https://github.com/lanl-ansi/WaterModels.jl>.
- Tasseff B, Coffrin C, Wächter A, Laird C (2019b) Exploring benefits of linear solver parallelism on modern nonlinear optimization applications. *arXiv preprint arXiv:1909.08104* .
- Verleye D, Aghezzaf EH (2013) Optimising production and distribution operations in large water supply networks: A piecewise linear optimisation approach. *International Journal of Production Research* 51(23-24):7170–7189.
- Wächter A, Biegler LT (2006) On the implementation of an interior-point filter line-search algorithm for large-scale nonlinear programming. *Mathematical Programming* 106(1):25–57.
- Zhang J, Zhu D (1996) A bilevel programming method for pipe network optimization. *SIAM Journal on Optimization* 6(3):838–857.
- Zheng F, Zecchin AC, Newman JP, Maier HR, Dandy GC (2017) An adaptive convergence-trajectory controlled ant colony optimization algorithm with application to water distribution system design problems. *IEEE Transactions on Evolutionary Computation* 21(5):773–791.

Appendix A: Derivation of $(P(r))$'s Dual

A straightforward method to derive the dual problem of $(P(r))$ is via Lagrangian duality, i.e.,

$$\max_h \min_{q^\pm \geq 0} \mathcal{L}(q^+, q^-, h) = \max_h g(h), \quad (38)$$

where \mathcal{L} is the Lagrangian of $(P(r))$ with dual variables h (for flow conservation constraints), and $g(h)$ is the Lagrangian dual function (to later be maximized). Following $(P(r))$, its Lagrangian is written as

$$\begin{aligned} \mathcal{L}(q^+, q^-, h) := & - \sum_{i \in \mathcal{J}} h_i d_i + \sum_{a:=(i,j) \in \mathcal{A}; i \in \mathcal{S}} \left[\frac{L_a r_a}{1+\alpha} (q_a^+)^{1+\alpha} - (h_i^s - h_j) q_a^+ \right] \\ & + \sum_{a:=(i,j) \in \mathcal{A}; i \in \mathcal{S}} \left[\frac{L_a r_a}{1+\alpha} (q_a^-)^{1+\alpha} + (h_i^s - h_j) q_a^- \right] + \sum_{\bar{a}:=(i,j) \in \mathcal{A}; i \in \mathcal{J}} \left[\frac{L_a r_a}{1+\alpha} (q_a^+)^{1+\alpha} - (h_i - h_j) q_a^+ \right] \\ & + \sum_{a:=(i,j) \in \mathcal{A}; i \in \mathcal{J}} \left[\frac{L_a r_a}{1+\alpha} (q_a^-)^{1+\alpha} + (h_i - h_j) q_a^- \right]. \end{aligned} \quad (39)$$

Equation (39) is highly separable in q_a^\pm . As such, minimization over q^\pm in Equation (38) is straightforward. To derive $g(h)$, it suffices to minimize each component of the second through fifth sums over their corresponding q_a^\pm while imposing nonnegativity on q_a^\pm . Note that all terms are of the form $\frac{b}{1+\alpha} (q_a^\pm)^{1+\alpha} + t q_a^\pm$, where $b > 0$ and the sign of t is unknown. There are two possibilities: if $t \geq 0$, the component is nondecreasing in q_a^\pm over $q_a^\pm \geq 0$, which implies its minimum is attained at $q_a^\pm = 0$. Otherwise, if $t < 0$, the function is decreasing

at $q_a^\pm = 0$, attains its minimum, then starts increasing. This minimum is attained at the stationary point $\hat{q}_a^\pm = \sqrt[\alpha]{-\frac{t}{b}}$. In this case, after reduction, the minimum value of the corresponding component is thus

$$\left(\frac{b}{1+\alpha} - b\right) \left(-\frac{t}{b}\right)^{1+\frac{1}{\alpha}} = \frac{-\alpha}{1+\alpha} \frac{(-t)^{1+\frac{1}{\alpha}}}{\sqrt[\alpha]{b}}. \quad (40)$$

Next, note that the second and third, as well as the fourth and fifth terms of the sums in Equation (39) can be paired such that the b coefficients of each term are the same, while the t coefficients are opposite. That is, one term (with nonnegative t) has a minimum at zero, while the other has a minimum equal to the right-hand side of Equation (40). Since the sign of t is unknown, $|t|$ is thus used instead to write $g(h)$ as

$$g(h) = -\sum_{i \in \mathcal{J}} h_i d_i - \sum_{a:=(i,j) \in \mathcal{A}: i \in \mathcal{S}} \frac{\alpha}{1+\alpha} \frac{|h_i^s - h_j|^{\alpha+1}}{\sqrt[\alpha]{L_a r_a}} - \sum_{a:=(i,j) \in \mathcal{A}: i \in \mathcal{J}} \frac{\alpha}{1+\alpha} \frac{|h_i - h_j|^{\alpha+1}}{\sqrt[\alpha]{L_a r_a}}. \quad (41)$$

Using a standard rewriting of the absolute value terms, the dual problem becomes equivalent to (D(r)).

Appendix B: Physical Interpretation of Strong Duality

Four sums appear in the objectives of (P(r)) and (D(r)), each having a unique physical connotation. This implies a physical meaning of the strong duality constraint. To begin, let this constraint be expanded as

$$f_P(q) - f_D(h) = f_1(q) - f_2(q) + f_3(\Delta h) + f_4(h) \leq 0. \quad (42)$$

Consider the first summation,

$$f_1(q) = \sum_{a \in \mathcal{A}} \frac{L_a r_a}{1+\alpha} [(q_a^+)^{1+\alpha} + (q_a^-)^{1+\alpha}]. \quad (43)$$

The terms involved are similar to those appearing in the head loss relationships, where $L_a r_a (q_a^\pm)^\alpha$ (conventionally in units of length) can be interpreted as the energy per unit weight of fluid lost to friction between the moving water and the interior wall of the pipe. Thus, up to a multiplicative constant, $L_a r_a (q_a^\pm)^\alpha q_a^\pm$ can be interpreted as the rate of heat transference (i.e., power) between the volume of water and the interior wall of the pipe. This sum can then be interpreted as all power losses from friction of the pipe walls.

Next, consider the second sum appearing in the primal problem (P(r)),

$$f_2(q) = \sum_{i \in \mathcal{S}} h_i^s \sum_{a \in \delta_i^+} q_a. \quad (44)$$

Here, each head h_i^s is static and can be viewed as the amount of energy per unit weight of water available for extraction from the reservoir. Thus, its product with the reservoir's (outgoing) flow can be interpreted, again up to a multiplicative constant, as the power generated by the reservoir. The sum of all contributions in Equation (44) is thus proportional to the power supplied to the water network.

Next, consider the first sum appearing in $(D(r))$, that is,

$$f_3(\Delta h) = \frac{\alpha}{1 + \alpha} \sum_{a \in \mathcal{A}} \frac{1}{\sqrt[\alpha]{L_a r_a}} \left[(\Delta h_a^+)^{1 + \frac{1}{\alpha}} + (\Delta h_a^-)^{1 + \frac{1}{\alpha}} \right]. \quad (45)$$

Here, each Δh_a^\pm denotes the difference in energy per unit weight between adjacent nodes. Each term thus represents, up to a multiplicative constant, the power loss along the pipe in the form of a head differential (i.e., *not* losses to heat from friction). The sum denotes the total loss in *usable* power across the network.

Finally, consider the second sum appearing in $(D(r))$, that is,

$$f_4(h) = \sum_{i \in \mathcal{J}} h_i d_i. \quad (46)$$

Here, each demand is fixed, while the energy per unit weight h_i at each junction can vary. Using an argument similar to that of Equation (44), this sum denotes, up to a constant, the power demanded across all junctions.

The strong duality constraint can then be thought of as encoding

$$(\text{frictional loss}) + (\text{realized loss}) + (\text{demand}) \leq (\text{generation}), \quad (47)$$

which implies the conservation of power, with an inequality replacing the traditional equality.

Appendix C: Modified Global Optimization Algorithm

Algorithm 2 modifies the algorithm of Raghunathan (2013) to define *this* study's global optimization algorithm. Portions that substantially modify the original algorithm are denoted by blue font. The algorithm begins in Line 1 by heuristically generating a feasible solution via Algorithm 4 of Raghunathan (2013) and storing the corresponding resistances r^* and initial objective η^* . It also initializes the set of encountered infeasible designs $\tilde{\mathcal{X}}$ to the empty set. Line 2 solves the root relaxation of (MICP-E) via a nonlinear programming algorithm (e.g., IPOPT of Wächter and Biegler (2006)). Lines 3 through 5 use the root relaxation's solution to generate initial linear outer approximations. In each cut, outer approximation points are chosen to coincide with maximal values of the corresponding nonlinear terms. Finally, since the root relaxation of (MICP-E) provides a lower bound on the optimal objective, Line 6 imposes this bound explicitly on (MIP-ER).

Line 7 begins the search of a MIP solver, where termination criteria comprises a minimal optimality gap or a time limit. Line 8 obtains the relaxation solution for the current node in the search tree. Line 9 computes the objective corresponding to this solution. Line 10 checks if the current branch and bound (BB) node's resistance choice solution is integer. If so, Line 11 obtains the corresponding active resistance parameters.

Algorithm 2 LP/NLP-BB algorithm for the global optimization of (MINLP)/(MICP-E).

- 1: $r^* \leftarrow \mathbf{InitialSoln}$ (Algorithm 4 of (Ragunathan 2013)); $\eta^* \leftarrow \sum_{a \in \mathcal{A}} L_a c_{ar_a^*}$; $\tilde{\mathcal{X}} \leftarrow \emptyset$.
 - 2: $(\hat{q}, \hat{h}, \Delta \hat{h}, \hat{x}, \hat{y}) \leftarrow \mathbf{Solve}$ (MICP-E) with $0 \leq x \leq 1$ using a nonlinear solver.
 - 3: $r_a^\pm \leftarrow \arg \max_{p \in \mathcal{R}_a} \{L_a p (\hat{q}_{ap}^\pm)^\alpha\}$, $\forall a \in \mathcal{A}$; $\tilde{Q}_{ar_a}^\pm \leftarrow \{\hat{q}_{ar_a}^\pm\}$, $\forall a \in \mathcal{A}$.
 - 4: $r_a^\pm \leftarrow \arg \max_{p \in \mathcal{R}_a} \{p (\hat{q}_{ap}^\pm)^{1+\alpha}\}$, $\forall a \in \mathcal{A}$; $\tilde{Q}_{ar_a}^{\text{NL}\pm} \leftarrow \{\hat{q}_{ar_a}^\pm\}$, $\forall a \in \mathcal{A}$.
 - 5: $r_a^\pm \leftarrow \arg \max_{p \in \mathcal{R}_a} \left\{ \frac{1}{\sqrt[p]{p}} (\Delta \hat{h}_{ap}^\pm)^{1+\frac{1}{\alpha}} \right\}$, $\forall a \in \mathcal{A}$; $\mathcal{H}_{ar_a}^{\text{NL}\pm} \leftarrow \{\Delta \hat{h}_{ar_a}^\pm\}$, $\forall a \in \mathcal{A}$.
 - 6: Add $\sum_{a \in \mathcal{A}} L_a \sum_{p \in \mathcal{R}_a} c_{ap} x_{ap} \geq \sum_{a \in \mathcal{A}} L_a \sum_{p \in \mathcal{R}_a} c_{ap} \hat{x}_{ap}$ to (MIP-E).
 - 7: **while** (MIP-ER) termination criteria is not satisfied **do**
 - 8: $(\hat{q}, \hat{h}, \Delta \hat{h}, \hat{x}, \hat{y}) \leftarrow \mathbf{Solve}$ the current nodal linear subproblem of (MIP-ER).
 - 9: $\hat{\eta} \leftarrow \sum_{a \in \mathcal{A}} L_a \sum_{p \in \mathcal{R}_a} c_{ap} \hat{x}_{ap}$.
 - 10: **if** $\hat{x}_{ap} \in \mathbb{B}$, $\forall a \in \mathcal{A}$, $\forall p \in \mathcal{R}_a$ **then**
 - 11: $r_a \in \{p \in \mathcal{R}_a : \hat{x}_{ap} = 1\}$, $\forall a \in \mathcal{A}$.
 - 12: $(\hat{q}, \hat{h}) \leftarrow \mathbf{Solve}$ (P(r)).
 - 13: **if** $\underline{q} \leq \hat{q} \leq \bar{q}$ and $\underline{h} \leq \hat{h} \leq \bar{h}$ **then**
 - 14: $r^* \leftarrow r$; $\eta^* \leftarrow \sum_{a \in \mathcal{A}} L_a c_{ar_a^*}$.
 - 15: $\mathcal{Q}_{ar_a}^\pm \leftarrow \tilde{Q}_{ar_a}^\pm \cup \{\pm \hat{q}_a\}$, $\forall a \in \mathcal{A} : \pm \hat{q}_a > 0$.
 - 16: $\mathcal{Q}_{ar_a}^{\text{NL}\pm} \leftarrow \tilde{Q}_{ar_a}^{\text{NL}\pm} \cup \{\pm \hat{q}_a\}$, $\forall a \in \mathcal{A} : \pm \hat{q}_a > 0$.
 - 17: $\tilde{\mathcal{H}}_{ar_a}^{\text{NL}\pm} \leftarrow \mathcal{H}_{ar_a}^{\text{NL}\pm} \cup \{\pm \Delta \hat{h}_a\}$, $\forall a \in \mathcal{A} : \pm \Delta \hat{h}_a > 0$.
 - 18: **else**
 - 19: $\tilde{\mathcal{X}} \leftarrow \tilde{\mathcal{X}} \cup \{\hat{x}\}$ (i.e., add a feasibility cut that removes \hat{x}).
 - 20: (repaired, r) $\leftarrow \mathbf{Repair}(r, n, \eta^*)$ (Algorithm 3 of (Ragunathan 2013)).
 - 21: **if** repaired **then**
 - 22: $r^* \leftarrow r$; $\eta^* \leftarrow \sum_{a \in \mathcal{A}} L_a c_{ar_a^*}$.
 - 23: $(\hat{q}, \hat{h}) \leftarrow \mathbf{Solve}$ (P(r)).
-

... Continuation of Algorithm 2.

```

24:       $\tilde{Q}_{ar_a}^\pm \leftarrow \tilde{Q}_{ar_a}^\pm \cup \{\pm \hat{q}_a\}, \forall a \in \mathcal{A} : \pm \hat{q}_a > 0.$ 
25:       $\tilde{Q}_{ar_a}^{\text{NL}\pm} \leftarrow \tilde{Q}_{ar_a}^{\text{NL}\pm} \cup \{\pm \hat{q}_a\}, \forall a \in \mathcal{A} : \pm \hat{q}_a > 0.$ 
26:       $\tilde{\mathcal{H}}_{ar_a}^{\text{NL}\pm} \leftarrow \tilde{\mathcal{H}}_{ar_a}^{\text{NL}\pm} \cup \{\pm \Delta \hat{h}_a\}, \forall a \in \mathcal{A} : \pm \Delta \hat{h}_a > 0.$ 
27:      end if
28:  end if
29:  else if (node index) mod  $J = 0$  then
30:      NodeCutsNew( $\tilde{\eta}, \hat{\eta}, m, (\hat{q}, \hat{h}, \Delta \hat{h}, \hat{x}, \hat{y}), \text{True}$ ).
31:       $r_a \leftarrow \arg \min \left\{ \hat{x}_{ap} \geq \frac{1}{|\mathcal{R}_a|} : p \in \mathcal{R}_a \right\}, \forall a \in \mathcal{A}.$ 
32:      (repaired,  $r$ )  $\leftarrow$  Repair( $r, \text{iter}^{\max}, \eta^*$ ) (Algorithm 3 of (Ragunathan 2013)).
33:      if repaired then
34:           $r^* \leftarrow r; \eta^* \leftarrow \sum_{a \in \mathcal{A}} L_a c_{ar_a^*}.$ 
35:      end if
36:  else
37:      NodeCutsNew( $\tilde{\eta}, \hat{\eta}, m, (\hat{q}, \hat{h}, \Delta \hat{h}, \hat{x}, \hat{y}), \text{False}$ ).
38:  end if
39:   $\tilde{\eta} \leftarrow \hat{\eta}.$ 
40: end while

```

Using these resistances, Line 12 solves (P(r)) to obtain its primal and dual solutions, \hat{q} and \hat{h} , respectively. This unique solution is then compared against the variable bounds of the original problem in Line 13.

If bounds are satisfied, \hat{x} is feasible for (MICP-E), and in Line 14, the incumbent solution is updated. If the solution is physically feasible, Lines 15 through 17 add outer approximations using the corresponding solution of (P(r)). Otherwise, if the design is *not* feasible, Line 19 adds a traditional combinatorial no-good feasibility cut. In Line 20, Algorithm 3 of Ragunathan (2013) is called in the attempt to heuristically recover a new feasible incumbent solution by “repairing” infeasibilities of the design \hat{x} , where n denotes the (fixed) maximum number of repair iterations to be used by the procedure. If the solution *was* repaired, as indicated in Line 21, then a new incumbent was found, which is updated in Line 22. Using the resistances from this

design, Line 23 solves $(P(r))$ to obtain the exact physical solution of the network. Then, in Lines 24 through 26, outer approximations are added to (MIP-ER) based on the physical solution corresponding to the design.

If the design solution is not integral, Line 29 serves as a possible entry point for adding outer approximations to (MIP-ER) and heuristically discovering new solutions. In this case, if the integer index of the BB node is divisible by some integer J , these routines are called. In Line 30, Algorithm 3 is called, which adds outer approximations based on the relaxation solution at the current BB node. This algorithm is described in Appendix D. Then, in Line 31, a heuristic resistance solution is prepared, which selects from active resistances in the current relaxation solution. The repair algorithm is then invoked on this (inexpensive but presumably infeasible) network design in Lines 32 through 34. For greater detail, this heuristic procedure is developed and elaborated upon by Raghunathan (2013). Otherwise, if both the design solution is fractional and the above heuristic is not activated, Algorithm 3 is called on Line 37, which conditionally refines (MIP-ER)'s outer approximations using the solution of the continuous relaxation at the current BB node.

Finally, on Line 39, the objective at the current BB node, $\hat{\eta}$, is stored as $\tilde{\eta}$ for use within methods of the next node. Specifically, both the current objective $\hat{\eta}$ and previous objective $\tilde{\eta}$ are used in a conditional step of Algorithm 3 to determine whether outer approximations should be added to (MIP-ER).

Algorithm 2 is highly similar to the algorithm of Raghunathan (2013) but differs in a few important respects. First, in Lines 3 through 5, initial outer approximations are based on the root relaxation of (MICP-E), whereas Raghunathan's algorithm uses the root relaxation of (MICP-R). Second, Raghunathan only applies outer approximations similar in form to Constraints (22), which correspond to convex head loss relaxations. Algorithm 2 extends this by adding outer approximations of terms appearing in the strong duality Constraint (27). Lastly, Line 30 ensures outer approximations will occasionally be added to (MIP-ER), whereas the conditions in Raghunathan's algorithm (and in their **NodeCuts** algorithm) are more restrictive.

In our study, implementations of the new and previous algorithms required some modifications, as necessitated by feature limitations of JUMP. First, the depth of a node in the branch and bound tree (m in Algorithm 2) is used as a parameter in both algorithms but is not easily accessible via JUMP. Thus, the number of unity-valued components of \hat{x} at a node in the BB tree is used instead. Additionally, a number of modifications are made to Raghunathan's algorithm to ensure fairer comparison with Algorithm 2. The most substantial of these are as follows: (i) initial outer approximation points are taken from the root relaxation of (MICP-E); and (ii) similar to Lines 29 through 35 in Algorithm 2, the heuristic *and* **NodeCuts** methods are called every J BB nodes. Aside from these changes, Raghunathan's algorithm is nearly reproduced.

Appendix D: Modified NodeCuts Algorithm

Algorithm 3 NodeCutsNew($\tilde{\eta}, \hat{\eta}, m, (\hat{q}, \hat{h}, \Delta\hat{h}, \hat{x}, \hat{y}), \text{Force}$)

```

1: if  $\left[ (\text{rand}([0, 1]) \leq \beta_{oa} 2^{-m}) \wedge \left( \left| \frac{\hat{\eta} - \tilde{\eta}}{\tilde{\eta}} \right| \geq K_{oa} \right) \right] \vee \text{Force} = \text{True}$  then
2:   for  $a \in \mathcal{A}$  do
3:     if  $\hat{y}_a \geq 0.5$  then
4:        $r_a \leftarrow \arg \max_{p \in \mathcal{R}_a} \{ L_a p (\hat{q}_{ap}^+)^{\alpha} \}$ 
5:       if  $\left| L_a r_a (\hat{q}_{ara}^+)^{\alpha} - \Delta \hat{h}_{ara}^+ \right| > \epsilon$  then  $\tilde{\mathcal{Q}}_{ara}^+ \leftarrow \tilde{\mathcal{Q}}_{ara}^+ \cup \{ \hat{q}_{ara}^+ \}$  end if
6:        $r_a \leftarrow \arg \max_{p \in \mathcal{R}_a} \{ p (\hat{q}_{ap}^+)^{1+\alpha} \}$ 
7:       if  $\left| \frac{r_a (\hat{q}_{ara}^+)^{1+\alpha}}{1+\alpha} - \hat{q}_a^{\text{NL}} \right| > \epsilon$  then  $\tilde{\mathcal{Q}}_{ara}^{\text{NL}+} \leftarrow \tilde{\mathcal{Q}}_{ara}^{\text{NL}+} \cup \{ \hat{q}_{ara}^+ \}$  end if
8:        $r_a \leftarrow \arg \max_{p \in \mathcal{R}_a} \left\{ \frac{1}{\sqrt[p]{p}} (\Delta \hat{h}_{ap}^+)^{1+\frac{1}{\alpha}} \right\}$ 
9:       if  $\left| \frac{(\Delta \hat{h}_{ara}^+)^{1+\frac{1}{\alpha}}}{(1+\frac{1}{\alpha}) \sqrt[p]{r_a}} - \Delta \hat{h}_a^{\text{NL}} \right| > \epsilon$  then  $\tilde{\mathcal{H}}_{ara}^{\text{NL}+} \leftarrow \tilde{\mathcal{H}}_{ara}^{\text{NL}+} \cup \{ \Delta \hat{h}_{ara}^+ \}$  end if
10:    else
11:       $r_a \leftarrow \arg \max_{p \in \mathcal{R}_a} \{ L_a p (\hat{q}_{ap}^-)^{\alpha} \}$ 
12:      if  $\left| L_a r_a (\hat{q}_{ara}^-)^{\alpha} - \Delta \hat{h}_{ara}^- \right| > \epsilon$  then  $\tilde{\mathcal{Q}}_{ara}^- \leftarrow \tilde{\mathcal{Q}}_{ara}^- \cup \{ \hat{q}_{ara}^- \}$  end if
13:       $r_a \leftarrow \arg \max_{p \in \mathcal{R}_a} \{ p (\hat{q}_{ap}^-)^{1+\alpha} \}$ 
14:      if  $\left| \frac{r_a (\hat{q}_{ara}^-)^{1+\alpha}}{1+\alpha} - \hat{q}_a^{\text{NL}} \right| > \epsilon$  then  $\tilde{\mathcal{Q}}_{ara}^{\text{NL}-} \leftarrow \tilde{\mathcal{Q}}_{ara}^{\text{NL}-} \cup \{ \hat{q}_{ara}^- \}$  end if
15:       $r_a \leftarrow \arg \max_{p \in \mathcal{R}_a} \left\{ \frac{1}{\sqrt[p]{p}} (\Delta \hat{h}_{ap}^-)^{1+\frac{1}{\alpha}} \right\}$ 
16:      if  $\left| \frac{(\Delta \hat{h}_{ara}^-)^{1+\frac{1}{\alpha}}}{(1+\frac{1}{\alpha}) \sqrt[p]{r_a}} - \Delta \hat{h}_a^{\text{NL}} \right| > \epsilon$  then  $\tilde{\mathcal{H}}_{ara}^{\text{NL}-} \leftarrow \tilde{\mathcal{H}}_{ara}^{\text{NL}-} \cup \{ \Delta \hat{h}_{ara}^- \}$  end if
17:    end if
18:  end for
19: end if

```

Algorithm 3 modifies the **NodeCuts** algorithm of Raghunathan (2013) to define this study's implementation. Portions that substantially modify the original are denoted by blue font. The method requires five parameters: $\tilde{\eta}$, the objective value of the previous BB node's relaxation solution; $\hat{\eta}$, the objective value at the current node; m , the depth of the current node; $(\hat{q}, \hat{h}, \Delta\hat{h}, \hat{x}, \hat{y})$, the relaxation solution at the current

node; and Force, a Boolean variable describing whether or not to force the addition of cuts. Line 1 begins by checking three conditions. First, a random number uniformly generated between zero and one is compared against the term $\beta_{oa}2^{-m}$, where β_{oa} is a positive parameter. This encourages cuts to be added near the top of the search tree. The second condition, $\left| \frac{\hat{\eta} - \tilde{\eta}}{\tilde{\eta}} \right| \geq K_{oa}$, computes the relative change in the objective between successive nodes and compares it with the positive constant K_{oa} . This encourages cuts to be added when the solution has significantly changed. Finally, Force can override the prior conditions, as used in Line 30 of Algorithm 2.

If conditions have been satisfied, the algorithm proceeds in Line 2 by looping over all arcs. In Line 3, if the relaxed flow solution along an arc is overall positive, cuts for positive flow are potentially added in Lines 5, 7, and 9. The reference resistances for each of these cuts, r_a , are independently computed in Lines 4, 6, and 8, where each corresponds to the maximum nonlinear term given the current relaxation solution. The conditionals on Lines 5, 7, and 9 imply these cuts will only be added if the relaxation solution deviates substantially (greater than a violation of some small constant, ϵ) compared to the solution of a corresponding nonlinear formulation. This limits the number of cuts being added by ensuring that only constraints with significant violations will be linearized. In Lines 11 through 16, the above process is analogously completed for arcs where flow along that arc is overall negative. In our study, parameters of Algorithms 2 and 3 coincided with those used by Raghunathan, namely, $\beta_{oa} = 5$, $J = 500$, $K_{oa} = 10^{-3}$, $n = 50$, and $\epsilon = 10^{-6}$.